Signature Page

For The Science Requirements Document

Title of Experiment: **Spacecraft Materials Microgravity Research on Flammability (SMμRF) Experiment**

Date:

Revision:

Principal Investigator	Signature	Date

PI's Address:

CONCURRENCE

NASA Glenn Research Center:

Project Scientist	Signature	Date

Project Manager	Signature	Date

Discipline Lead Scientist	Signature	Date

Discipline Program Manager	Signature	Date

NASA Headquarters:

Enterprise Discipline Scientist	Signature	Date

APPROVAL

Enterprise Lead Scientist	Signature	Date

SMµRF

Spacecraft Materials Microgravity Research on Flammability

Science Requirements Document

S. Olson
NASA Glenn Research Center
Principal Investigator

D. Hirsch
NASA White Sands Test Facility
Co-Investigator

SCIENCE REQUIREMENTS DOCUMENT

TABLE OF CONTENTS

`

List of Tables

List of Figures

Nomenclature

Acronyms

LOI
MOC
SDEP
SMµRF
ULOI

0.0 Executive Summary

NASA STD 6001 Test 1 is the major method used to evaluate flammability of materials intended for use in habitable environments of U.S. spacecraft. The method is an upward flame propagation test initiated in a stagnant environment and using a well-defined igniter flame at the bottom of a vertically mounted sample. A material passes this test if the vertical burn length is less than 15.2 cm (6 inches) and there is no evidence of transfer of burning debris. The test is conducted in the most severe flaming combustion environment (oxygen concentration, pressure) expected in the spacecraft, currently 30% oxygen at 10.2 psia.

Recent research has shown that current normal gravity materials flammability tests do not correlate with flammability in ventilated microgravity or partial gravity conditions. The materials selection for spacecraft is based on the assumption of commonality between ground test flammability results and spacecraft environments, which does not appear to be valid. To better understand the actual normal gravity flammability limits, a modified Test 1 protocol has been proposed that, as an alternative to qualifying materials as pass/fail in the worst-expected environments, measures the actual upward flammability limit (akin to the Limiting Oxygen Index (LOI)) for the material so that a more accurate assessment of the margin of safety of the material in the real use environment can be made. The method allows the option of selecting better or best materials based on the margin of safety, as opposed to what would be considered just “passing” from a flammability point of view.

A flight experiment is defined here to correlate normal gravity flammability test data with data under ventilated microgravity conditions. Rigorous correlations between ground test flammability data and data in ventilated spacecraft environments would allow selection of materials with increased fire resistance, and thus decrease the fire risk in space systems. The operational flexibility will also increase since the safety factors will be assessable.

1 Introduction

1.1 Background and Overview

The ***hypothesis*** to be tested in this research is that a material's flammability hazard in microgravity or partial gravity is at least equivalent to and may be greater than its flammability measured in normal gravity. If true, a factor of safety is needed for materials to 'de-rate' them for use in microgravity or partial gravity.

For future space missions, NASA is planning to increase the oxygen concentration and reduce the total pressure of the atmosphere in the Orion crew exploration vehicle, the Altair lander, and future lunar habitats [Campbell]. This atmosphere has the advantages of requiring a lower mass of inert gas (N_2), lowering vehicle internal pressures, and shortening or eliminating the pre-breathing time required to purge nitrogen from the bloodstream before Extra Vehicular Activity (EVA). However, an enriched oxygen atmosphere also has a significant disadvantage – increased flammability of materials.

One of the major lessons learned from the Apollo 1 fire is that it is impossible to eliminate all ignition sources [Lewis et al., 2007], so fire prevention is achieved in spacecraft through material control and the use of fire resistant materials. Since Skylab, the Space Shuttle and the International Space Station (ISS) have operated at normal sea-level conditions (air, 21% oxygen/79% nitrogen by volume at 14.7 psia total pressure) except for brief pre-EVA activities when oxygen levels are increased for a short period of time to 30% oxygen while the total pressure is lowered to 10.2 psia. Many of the materials now used in the Shuttle or on ISS are therefore only tested and rated to 30% oxygen at 10.2 psia.

The Crew Exploration Vehicle (CEV), Orion, and the lunar lander, Altair, are designed to operate from 8.0 psia to 14.9 psia and at a maximum of 30% and 34% oxygen concentration respectively. The transition from higher pressure, lower oxygen concentrations to lower pressure, higher oxygen concentrations will occur as exploration needs change from ISS crew exchange to Lunar missions. As the oxygen concentration increases, the cabin pressure decreases to follow the normoxic curve which keeps the partial pressure of oxygen constant at the normal atmospheric air equivalent of 0.21 atmospheres, or 3.09 psia. The partial pressure of oxygen in the spacecraft will be controlled to 2.6-3.1 psia, which creates a band of operating conditions on the hypoxic side of the normoxic curve.

NASA tests materials for flammability using NASA STD-6001 Test 1, which is an upward burning test at the worst-case atmospheric conditions in which the material will be used. Materials that do not self-extinguish after six inches of burning must undergo other special considerations and/or tests if they are to be used on spacecraft. Recently, a modified Test 1 has been evaluated [Hirsch references] to provide additional information about the flammability limits of the material and not just a pass/fail statement regarding its use in the worst-case atmosphere. This approach allows a better understanding of the margin of safety for the material in the real-use atmosphere.

In the modified procedure [Hirsch and Beeson, 2002], the oxygen concentration in Test

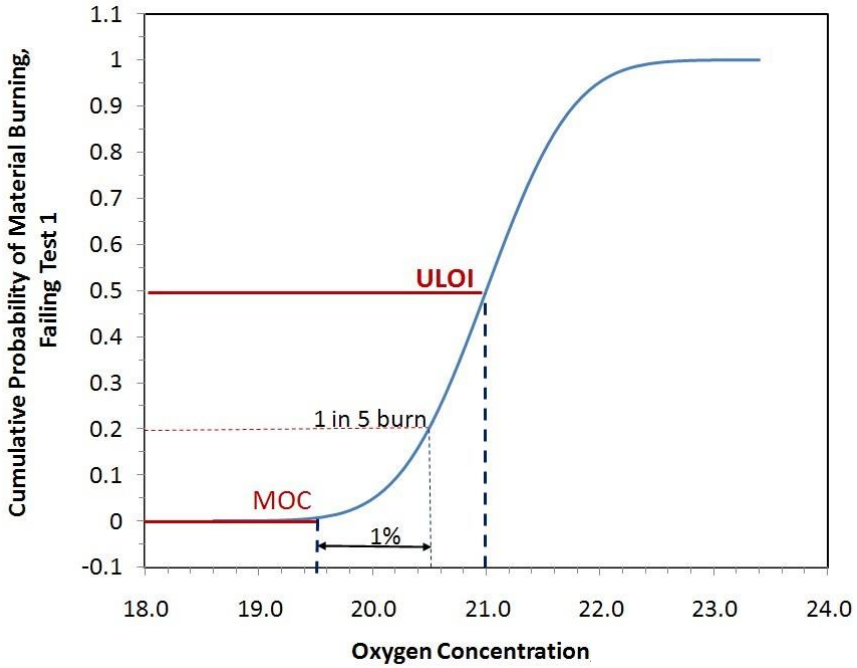

Figure 1. Near limit probability that a material will burn or not, with the ULOI and MOC indicated.

1 is successively reduced to identify the Upward Limiting Oxygen Index (1g ULOI) and the Maximum Oxygen Concentration (1g MOC) that consistently results in self-extinguishment of the material. The 1g ULOI is defined as the oxygen concentration at which a material passes the NASA STD 6001 Test 1 burn length criterion approximately half the time. The 1g MOC is defined as the oxygen concentration where at least five samples passed the burning criterion [NASA STD-6001] and where at least one sample failed in the environment that contained 1 percent more oxygen by volume. This is depicted graphically in Figure 1.

1.2 Results from Ground-Based Experiments

The microgravity tests were performed in a low-speed flow tunnel that provides 0-30 cm/s forced flow of gas (0-100% O_2 in diluent) through a 20 cm ID duct at 0-14.7 psia pressure. Flame images obtained in the facility are shown in Figure 2. The flow tunnel is mounted on a NASA Zero Gravity Research Facility drop rig bus [Olson, 1991]. The flow system includes a second gas reservoir such that oxygen concentrations (or another parameter such as diluent or extinguishing agent) can be changed during a test. A back pressure control valve maintains chamber pressure with flow at up to 14.7 psia.

For the material flammability tests, the switching of the flow between source bottles was timed so that the sample was ignited in an enriched oxygen concentration greater than the 1g ULOI, and the test oxygen level reached the sample shortly after release into zero gravity. The established flame then had ~ 5 seconds in which to respond to the new atmosphere by either extinguishing (0g MOC) or shrinking to a reduced burning state at the lower oxygen concentration. The lowest oxygen concentration where the flame survived to the end of the drop is considered the 0g ULOI. While some of these flames may extinguish given longer time, the limits provided by the Zero Gravity Research Facility tests are a conservative measure of the

limits in 0g. Note these limits are not identical to the 1g limits due to the intrinsic limitations of the drop time, but they are a reasonable comparison.

Tests were performed using a fuel sample taped to a sheet metal sample holder with an igniter wire on either the upstream or downstream end of the 5 cm wide by 10 cm long sample (Fig. 2). The flow was started before the drop to establish a steady flow speed and pressure in the tunnel prior to the drop rig release. The hot wire igniter was energized either in 1g or at release, depending on the objective of the test (flammability limit tests used 1g ignition; flame spread tests used 0g ignition). The microgravity period lasted 5.18 seconds – the first two seconds of which are typically used for 0g ignition and flame spread away from the igniter. When the drop rig reaches the bottom of the evacuated drop shaft and stops in the deceleration cart, the test section is vented to vacuum to extinguish the flame.

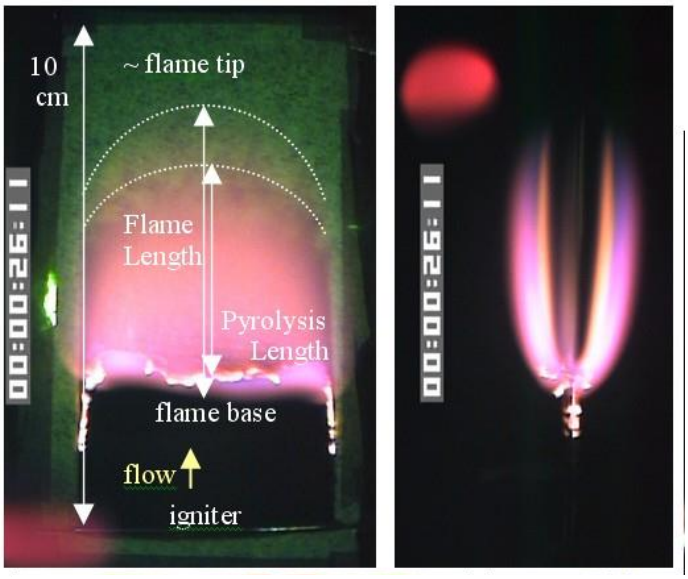

a) b)

Figure 2:
a) Front view of a microgravity concurrent flame spreading over Kimwipes® fuel sample. Test conditions are 24% oxygen, 30 cm/s, 6.4 psia (not near limit). The sample appears green due to the LED illumination.
b) Side view of same flame. The constant intensity red LEDs in both views was used to judge the actual flame brightness, since the camera was on auto-gain.

The fuels used to date include Kimwipes®, Ultem 1000®, Nomex HT90-40, Mylar G®, and 25 micron thick Acyrplen® (a.k.a. Shinkolite®). Kimwipes® have been extensively tested to expand the database for thin cellulose fuel that chars as it burns but is not treated for fire resistance. Front and side view images of a Kimwipes® burn are shown in Figure 2. With this fuel we can obtain flame spread and extinction data in the limited microgravity test time [Olson et al, 2008]. Acryplen, a similarly thin, fast buring non-charring fuel, was recently tested for oxygen, pressure and flow dependence [Olson and Ruff, 2009].

Figure 3. Front view pictures of 1g upward flame spread at the ULOI (WSTF Modified Test 1 with hot wire ignition). Samples are 5 cm wide in each image.

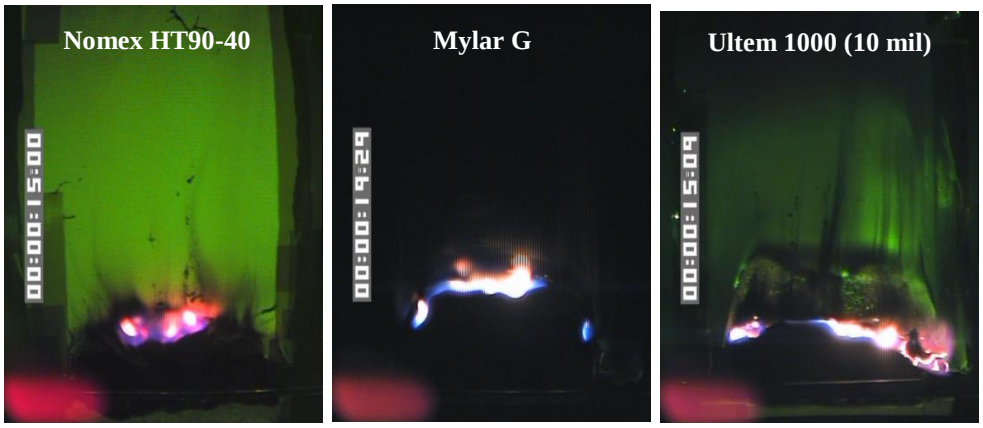

Figure 4. Front view pictures of microgravity concurrent flames with three different fuels samples at the ULOI. The concurrent forced flow velocity was 30 cm/s. The red LED in lower left is the same true brightness, giving an indication of the relative brightness between the flames. The green LED (for illumination) was not used for the Mylar as it caused too much specular reflection.

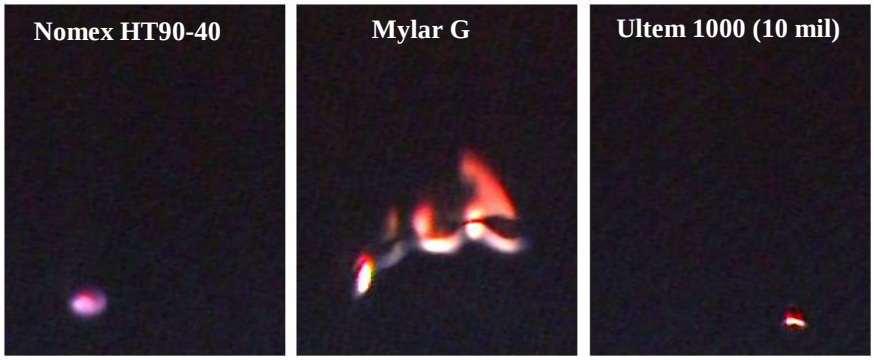

Figure 5. Front view pictures of lunar gravity concurrent flames for three different fuels samples at the ULOI.

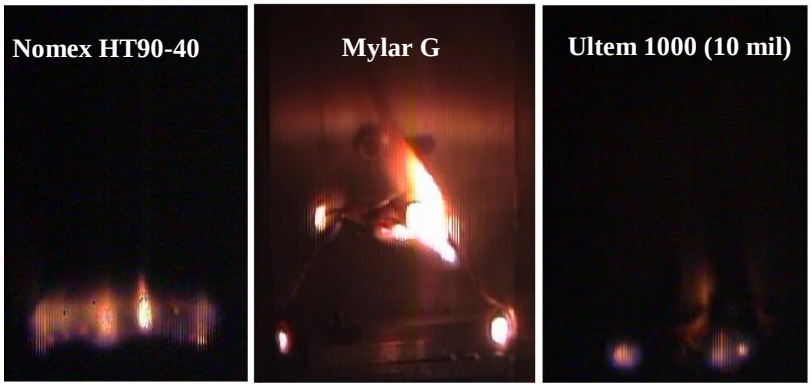

Figure 6. Front view pictures of Martian gravity concurrent flames for three different fuels samples at the ULOI just as the drop ends (t=5.18 s).

Three materials were evaluated for microgravity flammability limits (Figure 4) to compare with the 1g ULOI and 1g MOC (Figure 3). Ultem 1000® (fire retarded polyetherimide (PEI)) in 10 mil thick film is inherently flame-retarding, with self-charring characteristics, a very low smoke signature, very low smoke toxicity, and a low heat-release rate. Nomex HT90-40 is a 12 mil thick fire retarded aromatic nylon fabric which does not melt or drip as it burns. When exposed to a heat source, the Nomex fibers swell and seal the spaces between the fibers, stopping air movement through the fabric and thus inhibiting heat transfer through the fabric. Mylar G is a 5 mil thick plastic film made from polyethylene terephthalate. It is not fire-retarded, melts as it burns, and was selected primarily for its non-charring character.

Ignition and flame spread were recorded by two orthogonal color video cameras with automatic gain control; sample images are shown in Figures 3-6. Flame shape, size, and spread rate were measured using Spotlight software [Klimek and Wright, 2005]. Relative luminosity is compared between video frames using a constant brightness red LED in the corner of the flame images which also flashes at release.

Partial gravity was obtained using a centrifuge developed for use in a drop tower environment. The apparatus is subject to the usual constraints on size and volume for the Zero Gravity Facility at the NASA Glenn Research Center. The centrifuge consists of a flat circular base (turntable) and the chamber dome. Images of limit flames at lunar gravity are shown in Figure 5, and at martian gravity in Figure 6. (

1.2.1 Material Flammability Results

Materials flammability tests were conducted for three materials and the 1g ULOI and 1g MOC were compared with 0g values obtained at a concurrent flow of 30 cm/s, which is a reasonable maximum local spacecraft ventilation velocity [Sauers]. The limiting oxygen values for each fuel are found in Table 1. The near-limit flames are generally small and localized to the upstream edge of the material. We noticed that any distortion of the burned edge of the material, such as curling, swelling, or contracting, weakens the flame apparently by influencing the flow around the burned edge. Since oxygen transport is critical to microgravity flames, anything that reduces the free flow of oxygen past the sample will reduce the material's flammability.

Example flammability maps are shown in Figure 8 for Ultem 1000 and Figure 9 for Mylar, where the 1g limits are compared to low g test results over a range of flow, g, and oxygen concentrations. The observed minimum in the flammability curve is for concurrent flow at the highest velocities achievable in the drop rig (30 cm/s), so the remaining fuels were tested at 30 cm/s concurrent flow. The minimum g is near lunar gravity.

Figure 7 compares the flammability limits from Table 1 graphically, and evaluates the oxygen margin of safety for the 1g Test 1 data. The $\Delta O_2\%_{0g\text{-}1g}$ is defined here as the mean 0g limit minus the mean 1g limit in Equation 1 as follows:

Table I: Limiting Oxygen Molar Concentrations and Oxygen Margin of Safety for Different Gravity Levels

Fuel	**Mylar®** G 10.2 psia	**Ultem®** 1000 10.2 psia	**Nomex®** HT90-40 14.7 psia
1g ULOI	21.2	23.5	23.5
1g MOC	20.0	23.0	22.1
Martian ULOI*	18.0	22.0	19.9
Martian MOC*	17.0	21.1	19.0
Lunar ULOI*	15.6	21.0	21.0
Lunar MOC*	14.1	19.9	19.9
0g* ULOI*	17.0	24.0	23.0
0g* MOC*	16.0	23.0	22.0
Martian ΔO_2 %	**-3.1**	**-1.7**	**-3.35**
Lunar ΔO_2 %	**-5.75**	**-2.8**	**-2.35**
0g ΔO_2 %	**-4.1**	**0.25**	**-0.3**

$$\Delta O_2\%_{0g-1g} = \left(\frac{(0gULOI + 0gMOC)}{2}\right) - \left(\frac{(1gULOI + 1gMOC}{2}\right) \quad Eqn\ (1)$$

In this equation, the lowest $\%O_2$ at which the material burned in 0g for the full test was taken as the 0g ULOI; the maximum $\%O_2$ where the material extinguished during the test was taken as the 0g MOC. A positive $\Delta O_2\%_{0g\text{-}1g}$ means that the flame will propagate in 1g at lower oxygen concentrations than in 0g. Conversely, a negative $\Delta O_2\%_{0g\text{-}1g}$ means that the flame will propagate in 0g at a lower oxygen concentration than in 1g and would result in a reduced margin of safety.

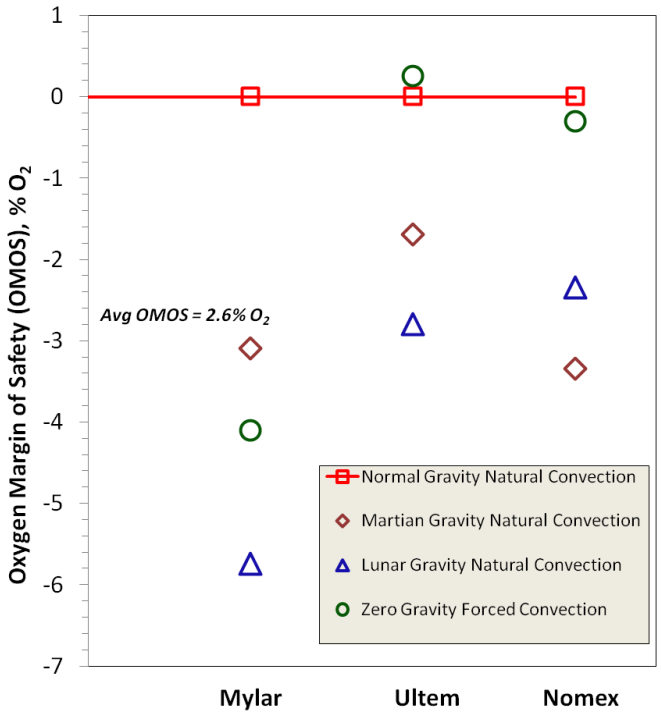

Figure 7. Oxygen Margin of Safety for four different gravity levels. The squares are normal gravity data which by definition has zero oxygen margin of safety since it is the test standard upon which materials are assessed. Martian, lunar, and microgravity oxygen margins of safety are generally negative by as much as -5.75% O_2 in molar concentration. The average 0g oxygen margin of safety for these three materials is -2.6% and the average Martian oxygen margin of safety is 2.7%.

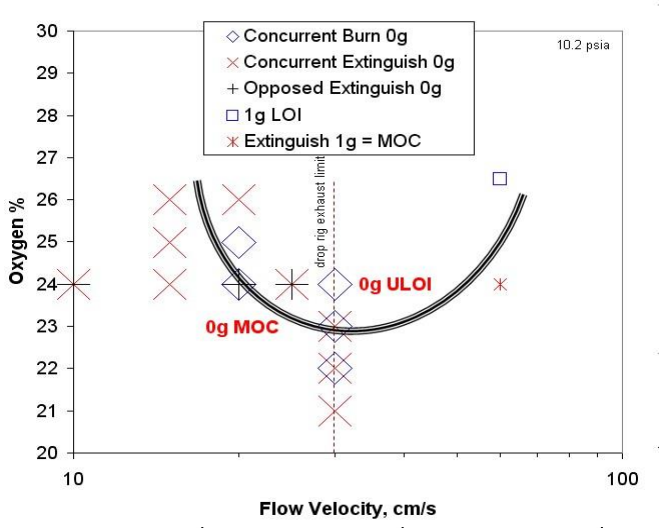

Figure 8 : Ultem 1000, 10 mil film, flammability map as a function of flow and oxygen %, with the pressure held constant at 10.2 psia. Most of the tests were conducted with concurrent forced flow velocity, but two were with opposed flow. The thick curved line indicates the approximate division between flammable and non-flammable conditions. Near the boundary the same conditions can yield different results due to the randomness of the flames and the samples curling which affects the airflow.

For example, Ultem® film is used aboard the Space Shuttle and the International Space Station, both of which have a nominal atmosphere of 21% oxygen ± 2% oxygen. In 1g, the mean flammability limit for Ultem® is 25.25%, which is at least 2.25% above the nominal range for the atmosphere. However, in 0g the mean flammability limit is 23.5%, which falls within the nominal range for the atmosphere, indicating the material could burn if ignited. The $\Delta O_2\%_{0g\text{-}1g}$=-1.75% is a significant negative margin of safety that needs to be considered when deciding if a material is safe for use in spacecraft. Mylar is even worse. The average of margin of safety for the three materials is $\Delta O_2\%_{0g\text{-}1g}$=-2.15% oxygen.

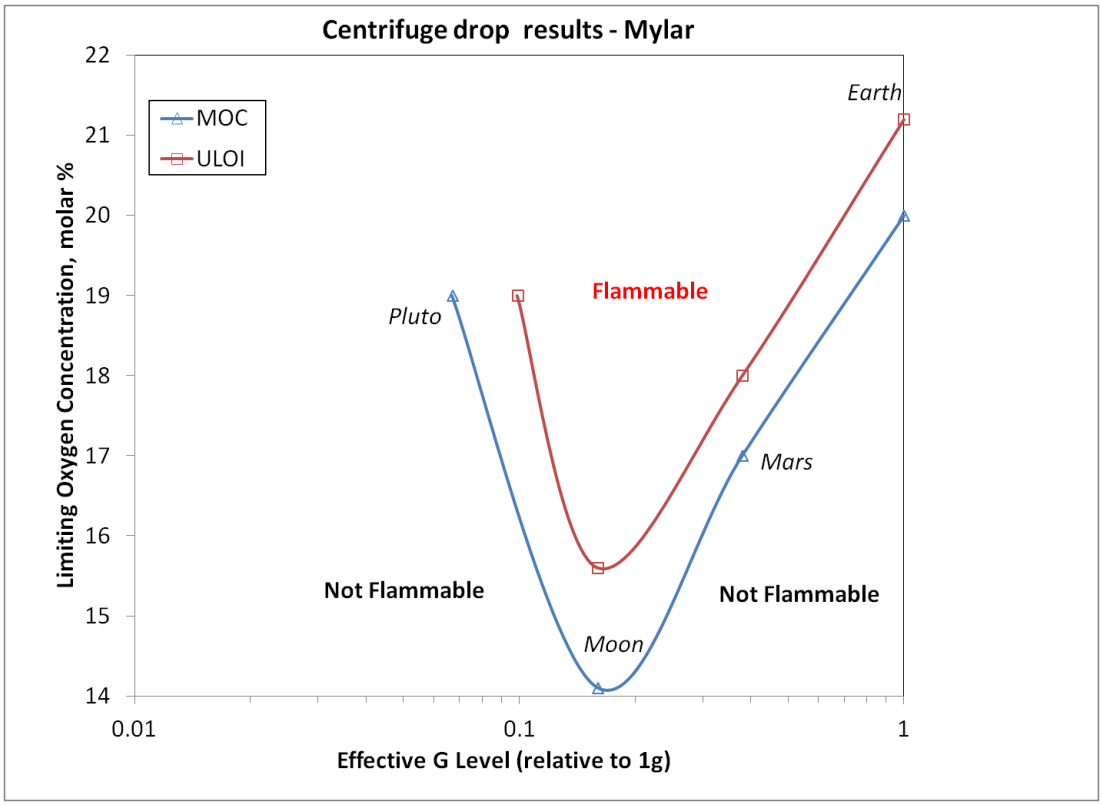

Figure 9. Limiting Oxygen Concentration as a function of g-level for Mylar. For a given oxygen concentration, there is range of g-levels which will permit the flame to be sustained.

As shown in Figure 7 and Table 1, the 1g flammability limits are generally not conservative for these materials as evidenced by the negative $\Delta O_2\%_{0g\text{-}1g}$, by up to -4% oxygen. For concurrent (upward) flow conditions, it is reasonable for materials to be flammable at lower oxygen concentration in low-g than in 1-g because in the absence of buoyancy, the heat loss due to convective flow is greatly reduced. As such, the flame doesn't have to release as much heat as in 1g to provide the same amount of heat flux to the unburned fuel. Thus, it is not surprising that the 0g flammability limits are lower than the 1g flammability limits, which is the general trend noted in Table 1. The evaluation of the magnitude of this $\Delta O_2\%_{0g\text{-}1g}$ for other materials is continuing for concurrent flammability limits, to be followed by evaluation of the limits for opposed flow.

1.2.2 Flame Spread Results

The 0g ULOI and 0g MOC measurements discussed in the previous section allow the difference between 1g and 0g oxygen flammability limits (or thresholds) to be quantified. However, this data does not quantify the difference in flammability at oxygen concentrations above the 0g MOC. As previously stated, atmospheres used in exploration vehicles will generally lie along the normoxic curve, i.e., the locus of ambient pressure/oxygen concentration combinations having the same oxygen partial pressure as standard sea level conditions. It would be useful to quantify material flammability along this curve so that trades between oxygen concentration and ambient pressure can be performed.

One way to determine relative flammability along the normoxic curve is to use flame spread as a measure of flammability. In this section, we describe the flame spread tests, develop correlations between forced flow velocity, oxygen concentration, and pressures to collapse the data onto a single curve, and finally extrapolate them to the normoxic condition.

Thirty concurrent and ten opposed flow flame spread tests were conducted with Kimwipes® to evaluate the effects of flow, pressure, and oxygen on the robustness of the flame. The flow velocity varied between 0 and 30 cm/s, the pressure varied between 3.6 and 14.7 psia, and the oxygen percentage ranged from 24 to 85 %. Spread rates were measured from the video for each test condition. Flame tracking was generally done with the edge view either manually or using an appropriate threshold value for the target. A more detailed report of these results can be found in [Olson and Miller, 2009].

Correlations were developed to capture the effect of all three of the variables (flow, pressure, oxygen) on the measured flame spread rate, and these correlations are shown in Figure 10 for opposed flow, and Figure 11 for concurrent flow.

For normal gravity, downward (opposed flow) flame spread over thin fuels, previous investigators found the flame spread rate correlated with $(O_2)^{0.9}(P)^{0.05}$, with oxygen in mole-fraction and pressure in atm. [Magee and McAlevy, 1971]. There was only a sight pressure dependence noted, so the primary influence on spread rate was from the oxygen concentration.

We found that our new data, as well as previous data from both normal and microgravity [Olson et al, 1988; Olson, 1987; Ferkul, 1989], were well-correlated by this relationship except near the quench limit where flow effects play a role. The results are shown Figure 10, where new data as well as previous data are shown. The spread rate increases nearly linearly with oxygen percentage, while the pressure effect is quite weak in this range. This is in contrast with Bhattacharjee *et al*., who showed a much stronger dependence on pressure for four-fold thicker fuel in a quiescent environment. Those tests were shown to be near-limit, where heat losses such as radiation become important. Indeed, even the near-limit data from [Olson, 1987; Olson et al., 1988] show a fall off from the correlation. Thus, the correlation can be viewed as a worst-case (*i.e.*, highest) prediction of spread rate for a given oxygen and pressure condition.

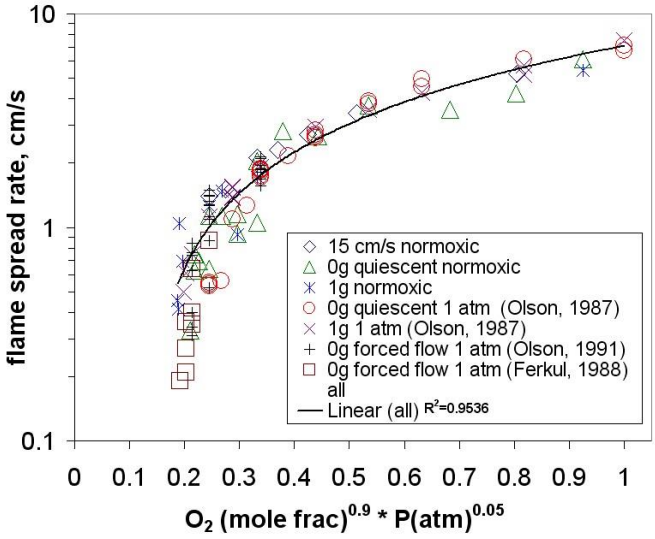

Figure 10: Opposed flow flame spread data for Kimwipes® , fit to an oxygen-pressure correlation based on Magee and McAlevy [13] for opposed flow under a variety of atmospheric and gravitational conditions. Flow velocity is not captured in this correlation due to the non-monotonic dependence of flame spread at low oxygen concentrations (<40%); below an optimum velocity the flame spread rate increases, and above that it decreases. Above 40% oxygen, the flame spread rate is independent of forced velocity.

For concurrent spread, there was no such correlation of experimental data in the literature that we could find, perhaps because in normal gravity the flame spread rate is often acceleratory. Ferkul [1993] did correlate his numerical predictions of spread rate as a function of oxygen and forced flow velocity in a polynomial expression, and noted the spread rate increases approximately linearly with either flow velocity or oxygen percentage.

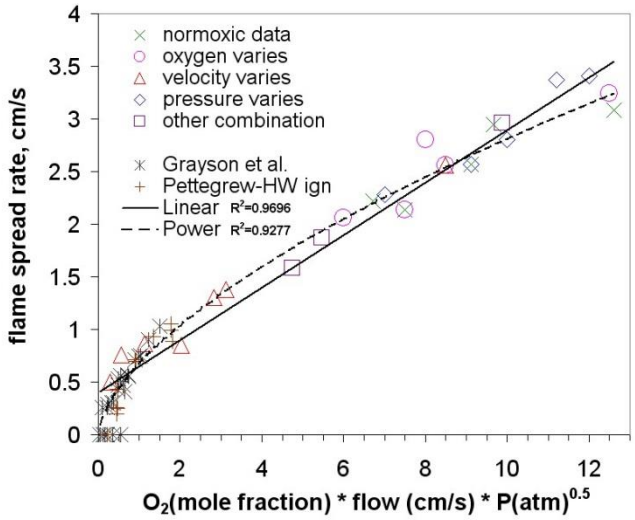

Figure 11: Concurrent flow flame spread correlation for Kimwipes® combining the effects of forced flow velocity, oxygen concentration, and ambient pressure. The symbols are sized to reflect the estimated error bars based on comparing top and bottom base spread rates. Data from [18,19] also shown for comparison. A linear fit to all the data is y=0.2498x+0.4038, with R^2=0.97. A power law fit to the data is $y=0.6763x^{0.6187}$ with R^2=0.93.

The best fit of the available experimental data was obtained by using the correlation parameter shown in Fig. 11, which captures the linear dependencies we observed for flow and oxygen, and a square root variation with

pressure. Here, all our data are shown, along with some earlier near-limit data from Grayson [1994] and Pettegrew [1996]. The normoxic data ranged from 24% oxygen at 12.8 psia to 85% oxygen at 3.6 psia, all at 30 cm/s flow. The oxygen varies from 24% to 50% oxygen at 10.2 psia and 30 cm/s. Velocity varies from 1 to 30 cm/s at 34% oxygen and 10.2 psia. Pressure varies from 5 to 14.7 psia at 40% oxygen and 30 cm/s. For most of the range, the spread rate depends linearly on the correlation parameter, but at very low near-limit values the data show a fall off from the linear fit, as predicted [DiBlasi, 1998]. A power law fit is shown for comparison in Figure 11.

More recent parametric flame spread studies were performed with a non-charring material. The non-charring thin fuel (25-micron thick Shinkolite™*) was tested in microgravity to compare with previous results with a charring thin fuel. Microgravity concurrent flame spread tests were performed in a low-speed flow tunnel to simulate spacecraft ventilation flows (7-31 cm/s). The tunnel atmosphere pressure and oxygen concentration was varied over a wide range (21-85% O_2, 5-16 psia).

Flame spread rate was measured to develop correlations that capture the effects of flow velocity, oxygen concentration, and pressure on the spread rate, as shown in Figure 12. The non-charring fuel exhibited a linear dependence on flow, similar to the charring fuel. However, the non-charring fuel had a weaker dependence on oxygen (square root versus linear for the charring fuel). The non-charring fuel was independent of pressure, unlike the square root dependence on pressure found for the charring fuel.

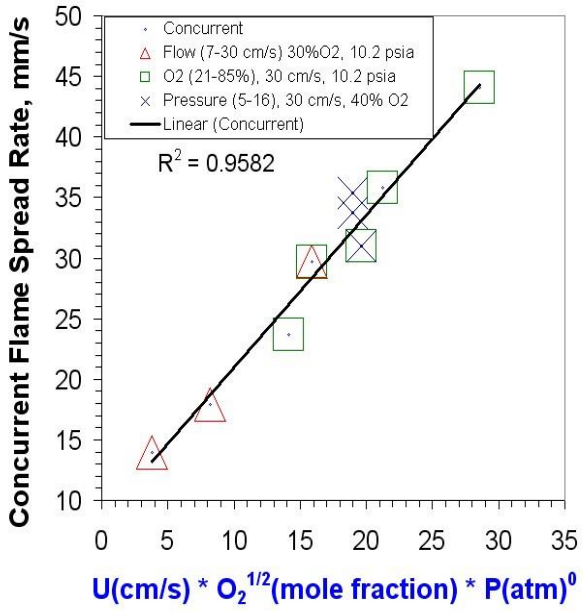

Figure 12: Concurrent flame spread correlation for Shinkolite™* combining the effects of forced flow velocity, oxygen concentration, and ambient pressure. The symbols are sized to reflect the estimated error bars based on comparing top and bottom base spread rates. A linear fit to all the data is y=1.261x+8.2998, with R^2=0.9582.

These results demonstrate that the effect of spacecraft atmosphere on concurrent flame spread depends on the class of material, so it would be prudent to develop fire safety protocols based on the most hazardous of the different correlations. The stronger dependence on oxygen concentration for both charring and non-charring fuels shows that the lower ambient pressure planned for exploration spacecraft and habitats does not offset the increased hazard of elevated oxygen.

Also, recall that the 0g MOC data in the previous section were obtained mostly in a concurrent flow configuration. Since the data in Fig. 10 and 11 show that the flame spread rates between concurrent and opposed flow are significantly different, it is plausible that the flammability limits in 0g may also be different, especially for materials whose limits lie at higher

oxygen concentrations along the normoxic curve, and should be investigated in future work.

We propose that the upward flammability limit (1g MOC) derived from Test 1 is essentially a limit dictated by the critical heat flux for ignition, where the heat flux from the flame is insufficient to sustain the burning. The similarity between the upward flammability limit and the lines of constant opposed flow flame spread rate can then be directly related. As was shown in [Olson et al., 2006], the limiting opposed flow flame spread velocity is directly related to the critical heat flux for ignition. Therefore, one of the lines of constant opposed flow flame spread rate will be the limiting spread rate, which is also the line of constant critical heat flux for ignition. This line would then correspond to the upward flammability limit of Test 1. If this hypothesis is verified by further experiments and analysis, it could help to understand the flammability limits derived from Test 1.

1.2.3 Flammability Maps

This proposal is directed toward improving NASA's Test 1 Upward Flammability Test by the evaluating the differences in the limiting oxygen concentration in normal and microgravity and partial gravity for upward flame spread rather than relying on a pass-fail criterion that provides no sense of a margin of safety.

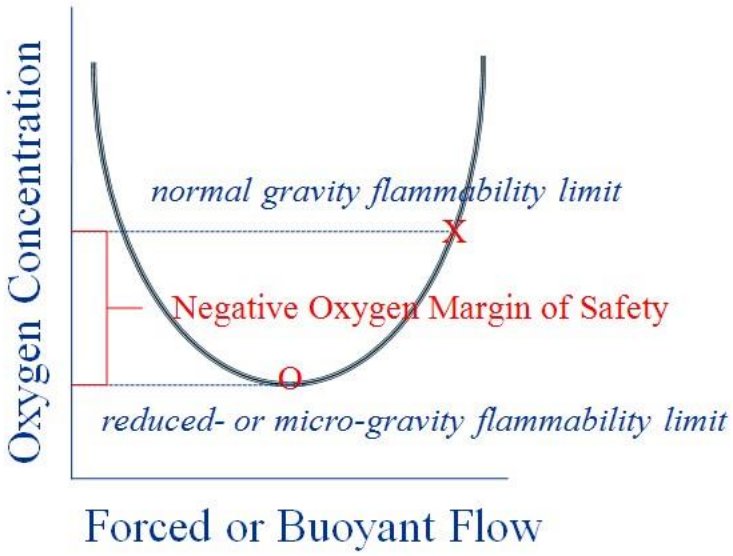

Figure 13: Conceptional Flammability Map showing the negative oxygen margin of safety.

The concept to be pursued in this effort is shown schematically in Figure 13. For each material tested, the normal gravity flammability limits will be evaluated based upon the modified Test 1 procedure [Hirsch references], and then the microgravity and partial gravity limits will be evaluated. The difference in these limits defines the negative oxygen margin of safety. Because buoyant flow is dominated by flame temperature, which in turn is primarily controlled by the oxygen concentration, different materials are expected to have similar limiting buoyant flow velocities. Similarly, in partial gravity, the minimum in the flammability map occurs as the flame transitions from the blowoff side of the flammability map to the quenching side of the map [Olson, 1991]. The velocity at which this occurs is hypothesized to also be similar for different materials, since it is also a gas-phase phenomenon. So the map, although it shifts vertically for different materials depending on their heat flux requirements, may not have a significant lateral shift. If so, it may be possible to estimate a reasonable value for the negative oxygen margin of safety for most materials. While pressure will also be varied for selected materials, its effect on the oxygen margin of safety is expected to be significantly less than oxygen concentration, based on data shown earlier.

Reduced gravity tests will be conducted starting with the pressure and oxygen concentrations corresponding to 1-g ULOI and MOC test results for the material. We will vary flow velocity and oxygen concentration to determine the flammability threshold for the material similar to Figure 13.

If the material is still burning at the end of the reduced gravity test time, it will fail the microgravity flammability criteria, whereas if it is extinguished at the end of the reduced gravity test time, it passes the microgravity flammability criteria. This criteria is inherently conservative since although some materials may extinguish if given a longer time, if it extinguished with the test time, it is clearly non-flammable in the atmosphere. Each extinction test will be repeated to verify it extinguishes.

Once the flammability map is identified from the test results, we will determine the minimum oxygen concentration in the flammability map, and, we will compare it to the 1g limits to evaluate the margin of safety for the material.

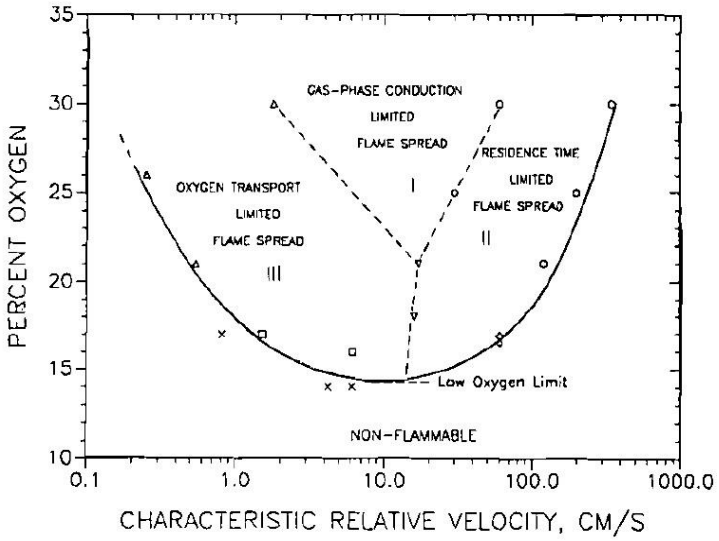

Figure 14a: Opposed flow flammability map for kimwipes (cellulose)

We can also use the reduced gravity flammability limits at the various flow velocities to evaluate safety factors at other flow velocities, which may provide valuable information for spacecraft ventilation design to improve spacecraft fire safety. Flow velocities in future spacecraft are currently planned for a wide range of 0 to about 1 m/s [NASA CxP 70024], but near burning surfaces flows would mostly be less than 30 cm/s. With this data, existing ISS and future CEV computational fluid dynamics of spacecraft flow velocities could be used to identify most-at-risk zones where flame propagation of materials qualified in 30% oxygen at 10.2 psia is possible.

The fundamental improvement in this proposed modified test method is based upon the hypothesis that all materials exhibit a similar flammability boundary as a function of oxygen and flow. The hypothesis that there may be a common negative oxygen margin of safety for many materials is based upon two fundamental concepts of material flammability.

The first concept is that of a critical heat flux for ignition. If we treat flame spread as a process of continual ignition, then if the flame does not provide adequate heat flux, the next section of fuel will not ignite and the flame will extinguish. This assumes, of course, that adequate ignition energy was supplied to ignite the material initially.

The critical heat flux for ignition is strongly influenced by convection. Increasing convective heat transfer ahead of the marginal concurrent flame should allow the flame to survive at the higher convective heat transfer. On the other hand, reducing convective heat

transfer may cause the flame to extinguish.

The second concept is that the heat release rate is proportional to the oxygen consumed [Huggett]. The oxygen consumption is limited by residence time on the blowoff side of the flammability map (Damkohler number effect), and by the ambient oxidizer flow rate on the quenching side of the flammability map [Olson, 1991]. Initially increasing convection will increase heat release as more oxygen is available for reaction. With higher convection comes reduced residence time, which may not allow the oxygen to fully react and release the maximum heat. This will counteract the effect of increased heat convection. An intermediate convective heat transfer rate that allows adequate time for chemical reaction will provide an optimum flammability, and correspond to the minimum in the flammability map.

In normal gravity testing, buoyant convection is high, and provides significant convective heat flux. However, there is a large amount of unburned oxygen that passes through the flame zone due to insufficient residence time for reaction. Reducing convection and allowing more time for chemical reaction can increase the material's flammability. It is this effect that all materials are hypothesized to have in common.

The only fuel-inherent property in the discussion above is that of the critical heat flux for ignition. The critical heat flux for ignition will dictate the limiting oxygen index, or vertical shift in the plot in Figure 13. In that case, the delta between normal gravity and microgravity limits (the negative oxygen margin of safety) will be similar for all fuels although the actual limiting oxygen concentration will be different. The opposed flow negative oxygen margin of safety for cellulose is approximately 2.5% as shown in Figure 14, in good agreement with the average of 2.15% for the three materials tested above. The relationship between the critical heat flux for ignition (from ELSA [Olson et al, 2005] inverted cone calorimeter tests) and the quantitative upward material flammability limits will be examined for the materials tested in this proposed work. It may be possible to relate them directly.

1.2.4 Geometry Considerations

Various materials have been tested to date. Polymethylmethacrylate (PMMA) and polyoxymethylene (POM) in different forms and shapes are reported in this paper. Both of these materials are non-charring, which is desirable for the intended flight experiment so that the same material can be re-ignited and tested at a different condition without the crew needing to open the chamber to change out the fuel. Additional desirable material characteristics for the flight experiment are a non-melting, non-swelling, non-deforming fuel so that the fuel shape remains the same (except for regression) during repeated tests.

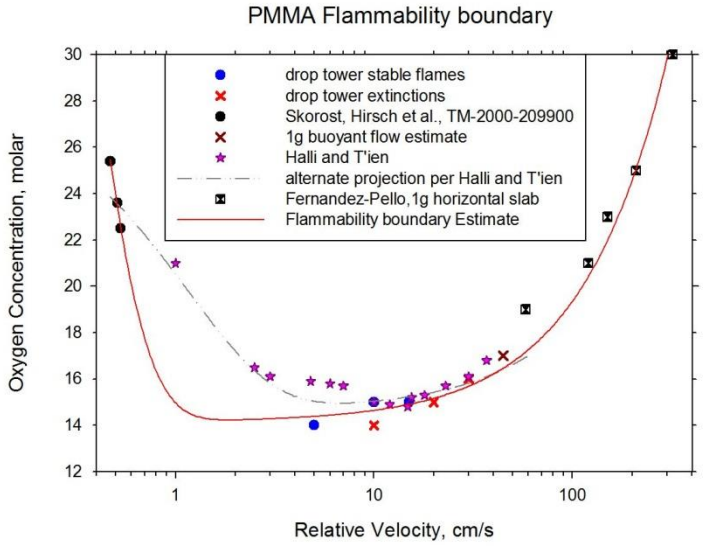

Figure 14b: Flammability boundary for PMMA, limit data from different sources. Note the uncertainty at low flow rates.

Clear PMMA spheres, rods, and sheets have been tested. In addition, extruded and cast rods are

compared. The primary difference in the two manufacturing processes is observed in the burning behavior. Extruded PMMA, having lower molecular weight chains that are generally aligned in the extrusion flow direction, melts readily into a low viscosity fluid which drips in normal gravity. Cast PMMA on the other hand, has a high molecular weight with random chain orientation, so its melt viscosity above the glass transition is high and generally does not drip in normal gravity. It will sag, however, if the sample is large and given enough burn time. White POM spheres, rods, and sheets have been tested. This material melts and drips in normal gravity, similar to extruded PMMA.

Figure 15 shows microgravity flame images from the different fuels and geometries tested in 1 atmosphere in a 5 cm/s air flow. Green LEDs are used for ambient illumination. For PMMA (Fig. 15 a-e), the flame is blue with an inner soot layer that is more prevalent for cast samples than the extruded sample.

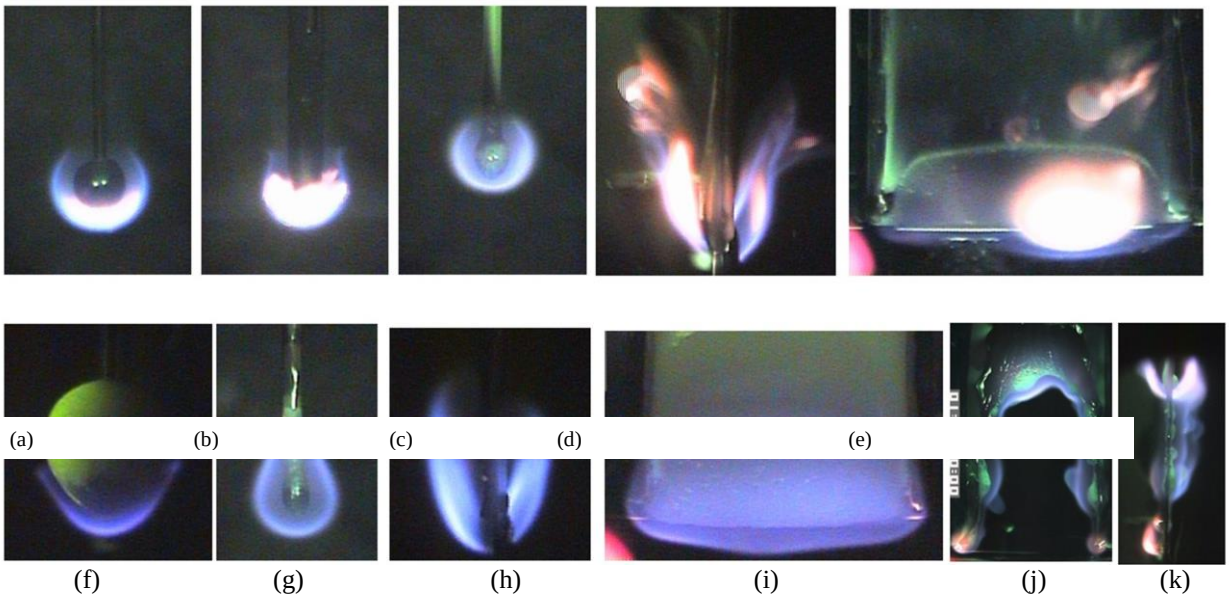

Figure 15. Microgravity flames of PMMA (a-e) and POM (f-k) burning in 5 cm/s air flow, in different geometries. All images same magnification except as noted. Orthogonal views from same time.
PMMA: a) 1 cm diameter cast sphere; b) 1/8" extruded rod; c) ¼" cast rod; d) and e) 0.9 mm cast sheet, orthogonal views.
POM: f) 2.5 cm diameter sphere; g) 1/8" rod; h) and i) 1.5 mm thick sheet, orthogonal views; and j) and k) thin film (44% size of other images).

Interestingly, the extruded rod configuration "drip-extinguishes" in normal gravity in 21% oxygen. This occurs when a sufficiently large amount of molten material drips, carrying away fuel and energy from the flame. The flame size is similar for the sphere and rods, but the sheet flame is longer and less uniform (not 2D) than the axisymmetric geometries. Vapor jetting is most prevalent for the cast rod and the sheet materials. In addition, the very thin 5 cm wide sheet warped during the test which would have perturbed the flow if re-used in subsequent tests.

For POM (Fig. 15 f-k), the flames are all blue and melting is noted in all fuel geometries. The sphere in Fig. 15f became egg-shaped during the 1g portion of the burn. The rod material drips in normal gravity, and has the tendency to drip-extinguish (noted in 1 drop test and also during 1g testing at WSTF). The thicker sheet material (Fig. 15 h-i) sags slightly but is otherwise fairly 2D whereas the thin film material melts into a series of droplets around the perimeter of the sample holder (Fig. 15j) creating a very non-uniform flame spread that is augmented by the surface tension driven melt-flow of the material.

Selected tests are analyzed for flame length, width, flame standoff distance, and ratios of these quantities. Flame size and spread rate information will be used to determine camera imaging requirements for the flight experiment. The data is shown in Figure 16 for four tests at 5 cm/s flow velocity. In Figure 16a, the data for the 1 cm (cast) PMMA sphere (shown in Figure 1a) shows that the flame reaches a steady overall size (length and width) within 1.5 seconds, but the standoff distance is gradually increasing with time as the interior of the fuel heats up and the surface energy balance determines that the flame heat flux back to the surface can be reduced as the conduction in depth is reduced. The flame thus slowly stabilizes further from the surface. It is also noticed that the ratios of L/W and standoff/sphere radius are close to unity for this test.

Figure 16b shows the data for the 1/4" (0.635 cm) cast PMMA rod (shown in Figure 15b). This material exhibited more size fluctuations due to the fuel vapor jetting in the sooty stagnation region. This increased vapor jetting may be due to material differences (the cast PMMA materials were not from the same vendor), or it could be due to the geometry and/or size differences. The standoff distance is most affected by the local vapor jetting. The standoff to radius ratio is ~2:1 in contrast to the 1:1 ratio for the sphere. but the overall flame size and aspect ratio (~1:1) are similar to the sphere. The flame shape at the downstream end differs with the geometry, with the flame curving inward to envelope the spherical sample in contrast to the flat slightly flared flame tips around the rod.

Figure 16c shows the data for the 1/8" (0.318 cm) extruded PMMA rod (shown in Figure 15c). The flame is smaller for this smaller diameter rod, but not as much as one would expect from the factor of two difference in rod size, and the L/W aspect ratio is again 1:1. In this test, the material melts and forms a larger diameter molten ball at the tip. The molten tip changes from a taper in 1g to a growing oval of increasing diameter during the drop, so the standoff distance from this changing surface at the stagnation region could not be measured if the molten material could not be seen (in 1g and early in 0g). The molten material tip moves more than 4 mm during the drop, so not accounting for its motion will lead to an incorrect trend in standoff distance. By the end of the test the oblong molten ball is 7.1 mm across, more than twice the diameter of the rod. The flame shape reflects this by resembling the flame around the sphere more than the flame around the rod. Interestingly, the standoff to rod radius ratio is ~ 2:1, which is the same as the ¼" rod, but the standoff to droplet radius ratio is 0.8:1, much like the sphere.

Figure 16d show the data for the 1/8" (0.318 cm) Acetron (POM) rod (shown in Figure 15g). After the transition to zero g, which takes less than 2 seconds, the flame begins to grow in both length and width, all while exhibiting whole-flame oscillations at a slow frequency of approximately 2 Hz. This oscillation is clearly visible in the flame standoff distance measurement. The cause of the oscillation is not clear, but may be due to waves of viscous molten liquid movement along the rod caused by the material shape change from 1g to 0g. This shape change is much more subtle than for the extruded PMMA sphere (compare Fig. 15c and 15g), and the final POM rod is 5.5 mm across from its intial 3.2 mm diameter.

Since the flame is growing in this test, it is possible to measure the spread rate. Both flame tips were tracked in normal gravity and through the drop test, as shown in Figure 17. The flame is spreading steadily at a rate of approximately 1.85 mm/s in normal gravity. After release into microgravity, the flame tips retract for a few seconds until the flame shape stabilizes (see Figure 16d) and the flame tips begin to propagate once again. Spread rates in microgravity (1.1 mm/s) are lower than in normal gravity, and the flame tips do not surpass the fuel positions they

reached during normal gravity. Since the flame is propagating over preheated fuel during the drop, it is difficult to conclude that this is steady spreading in microgravity from this short test. Work to model the solid-phase temperature field in a spherical geometry is underway [12]

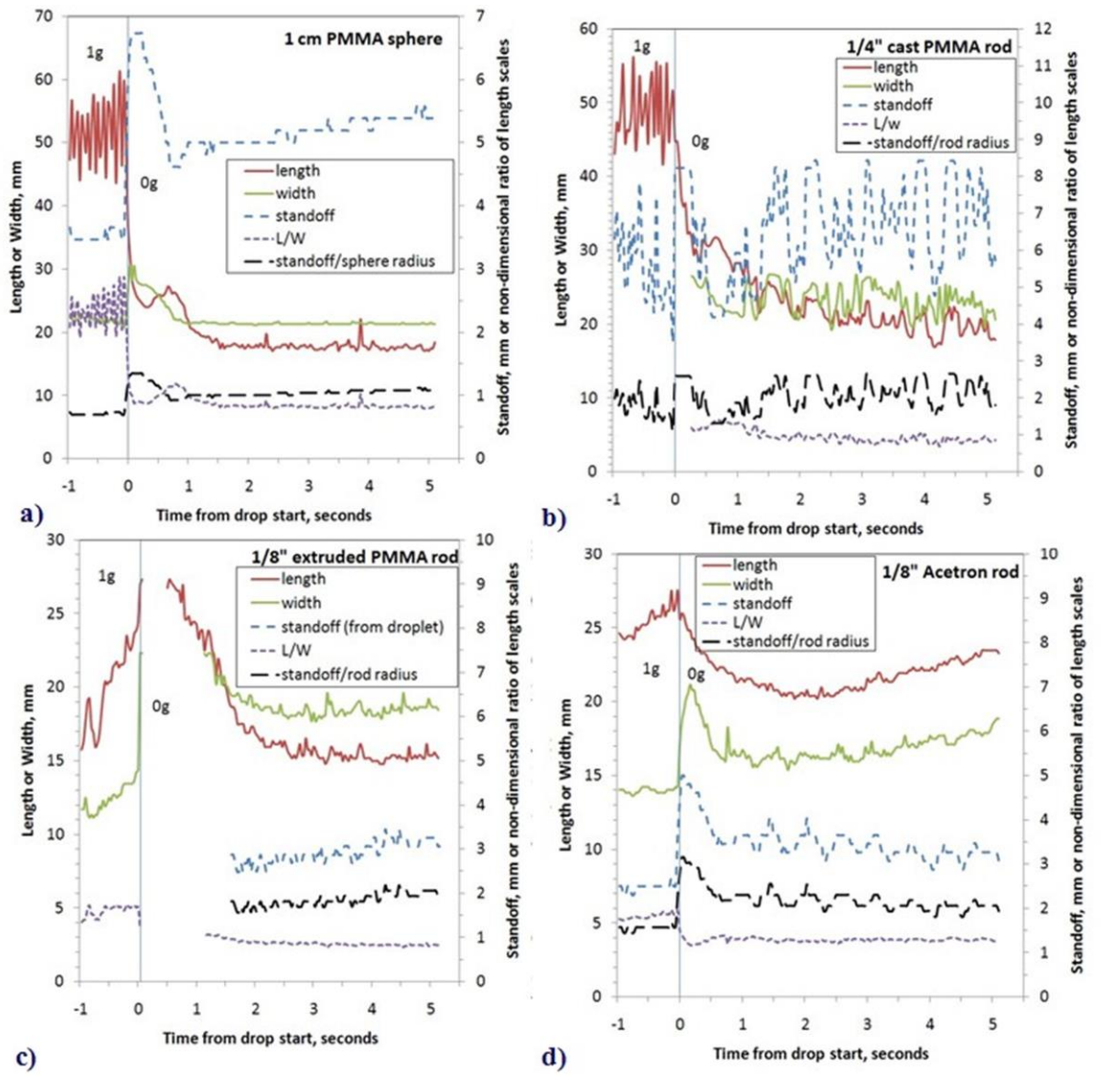

Figure 16. Flame size measurements as a function of time, from 1 second before the drop start through the end of the drop for each of 4 material/geometries as indicated on the graphs. Flow velocity is 5 cm/s in all 4 tests. Flame length and width are plotted on the left axis with solid lines (red and green), and the flame standoff distance and ratios of Length to Width and Standoff/Initial radius are plotted on the right axis with dashed lines (blue, purple, and black). Missing data is due to image bloom where tracking could not be done at the start of the drop in some tests. a) 1 cm PMMA sphere (cast); b) ¼" cast PMMA rod; c) 1/8" extruded PMMA rod; d) 1/8" Acetron (POM) rod.

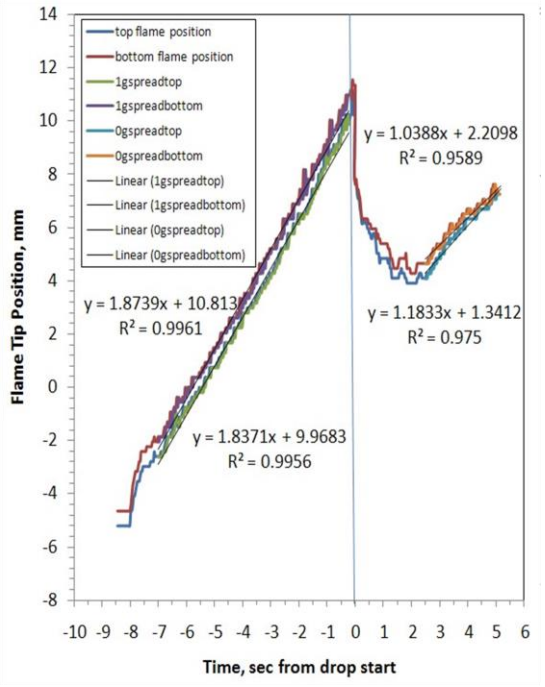

Figure 17. Flame tip positions as a function of time before and after the drop, showing the flame propagation along the Acetron (POM) rod. Linear fits are shown to determine spread rates.

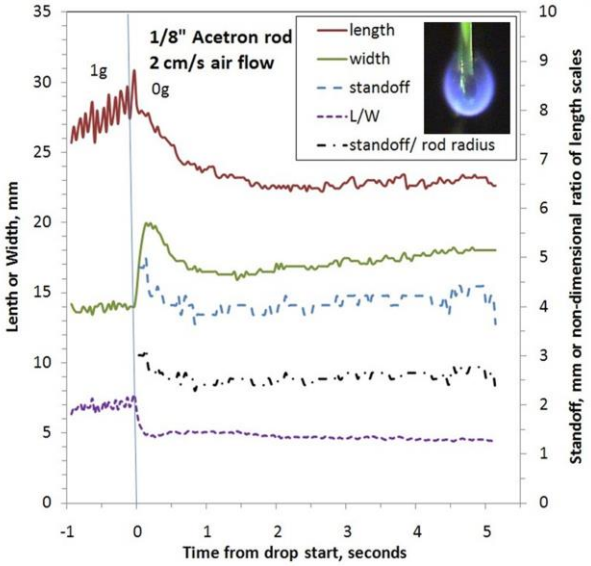

Figure 18. Flame size measurements as a function of time, from 1 second before the drop start through the end of the drop for a 1/8" Acetron (POM) rod at 2 cm/s air flow. The flame appearance is shown in the legend. Flame length and width are plotted on the left axis with solid lines (red and green), and the flame standoff distance and ratios of Length to Width and Standoff/Initial radius are plotted on the right axis with dashed lines (blue, purple, and black).

To examine how flow affects the flame spread, a test with the 1/8" POM rod was conducted at a lower flow rate of 2 cm/s. The flame image is shown in the inset to Figure 18. The flame is more spherical compared to Figure 15g, and the tips are significantly fainter than the stagnation region, whereas in Figure 15g the tips are quite sharply defined. The flame is also not spreading, as shown in Figure 18. The flame length is steady while the flame width is increasing slightly with time. The standoff distance is steady, but larger than for 5 cm/s, and not showing the oscillations that were persistent at 5 cm/s. The flame size is nearly identical at the two flow rates, and aspect ratio L/W is still close to unity, but the non-dimensional standoff distance S/R is significantly larger at 2 cm/s (2.66) than at 5 cm/s (2.1).

The results of the flame analyses are summarized in Table 2, including estimates of stretch rate and Reynolds number for each test.

Only limited extinction limit data has been obtained to date, but a few observations can be made. For extruded PMMA rods, the extinction limit in 0g is lower than in 1g due to the propensity of the material to drip extinguish. In 1g, the 1/8" sample drip extinguished in air, but during a drop in air at 5 cm/s, the sample burned steadily. Cast PMMA rods and cast PMMA spheres continued to burn at low velocities (rods 2-4 cm/s, spheres at 2 cm/s [12]) at oxygen concentrations down to 16% O_2. These values are close to the 1g hot wire ignition limit of 15.7% O_2 for cast PMMA rods [13]. Cast PMMA spheres burned steadily at 17% O_2, 28.5 cm/s but extinguished 16% O_2 at both 14 cm/s and 28.5 cm/s. The extinction was clearly a blow-off type at 28.5 cm/s, but is not clearly blow-off or quenching at 14 cm/s – the flame just fades away overall. It should be noted that fuel preheating was not the same in each test, so that may affect these observed extinction limits. In addition, the available 5.2 seconds of microgravity

Table 2: End of Drop Flame Dimensions and Non-dimensional measurements

Measurement\ Material	¼" cast PMMA rod	1 cm diameter PMMA sphere	1/8" extruded PMMA rod	1/8" POM rod 5 cm/s	1/8" POM rod 2 cm/s
Length, L, mm	20.7	18.7	15.5	24.0 increasing	23.19
Width, W, mm	22.3	21.3	18.5	18.6 increasing	18.01 increasing
Standoff, S, mm	7.5	5.4	2.9	3.3 oscillating	4.2
Initial radius, R, mm	3.175	5	1.59	1.59	1.59
L/W	0.93	0.88	0.84	1.29	1.29
S/R	2.10	1.03	2.00	2.1 oscillating	2.66
Final sample 'radius', mm	3.175	5	3.55	2.75	2.6
Effective radius, R', mm	10.675	10.4	6.45	6.05	5.8 decreasing
Effective stretch rate, $3\sqrt{2}\,U/R'$, s^{-1}	7.0	7.2	11.6	12.4	4.41
Re, $U(2R')/\nu$	68.0	66.2	41.1	38.5	17.32

is a very short time, and longer test times (i.e. a flight experiment) are needed to determine the long term viability of these near-limit low velocity flames. More testing is planned.

Similar rod samples (4.5 mm diameter) were tested aboard the Mir space station [14,15] using POM and extruded PMMA rods. A comparison between the flames in Mir and the drop test flames is shown in Figure 19. Conditions are not identical, as noted in the caption, but general trends can be observed. For the PMMA samples (Fig. 19 a-c), it is clear that the drop test flame is more blue, and the molten ball at the end of the rod is significantly smaller. The flame is also smoother than the Mir tests, indicating lower vapor jetting, which is known to perturb the flame symmetry. The Mir tests are sootier, which may be due to the longer burn times, which allows more fuel preheating and thus less heat loss to the solid. In addition, the oxygen levels were higher, which would result in higher flame temperatures, increased fuel vaporization, and thus a larger fuel-rich region, all of which contribute to increased sooting. The POM flame (Fig. 19 d-e) is smaller and shorter in the drop test, and again the molten ball is less developed.

The only reasonably comparable spread rates are the POM drop test at 1.1 mm/s (Figure 17) compared to 0.4 mm/s reported for the flame shown in Figure 19e [14]. Since the Mir test was at a higher flow rate and a higher oxygen concentration and yet had a lower flame spread rate, it can be concluded that the fuel preheating from the 1g portion of the burn (discussed above) substantially accelerated the flame spread rate during the drop test. The rod is smaller for the drop test, but it is likely this was much less a factor than the preheating.

These Mir tests [14] have implications for future flight experiments. Of note, the diameter of the molten ball generally did not reach a steady size during the tests, which generally lasted for hundreds of seconds. It is better to select a material that does not form a molten ball, such as cast PMMA. A material that is thick enough (thicker than 4.5 mm in diameter) so as not to bend is also a good choice. Noticeable rod bending is even visible in the drop test in Figure 19d. In one Mir test, the initial rod was bent by previous heating from an adjacent test, so the rod was ignited on the side where the igniter could reach. The flame propagated upstream to the tip of the rod and burned backward from there. The fuel burning behavior was less like a concurrent

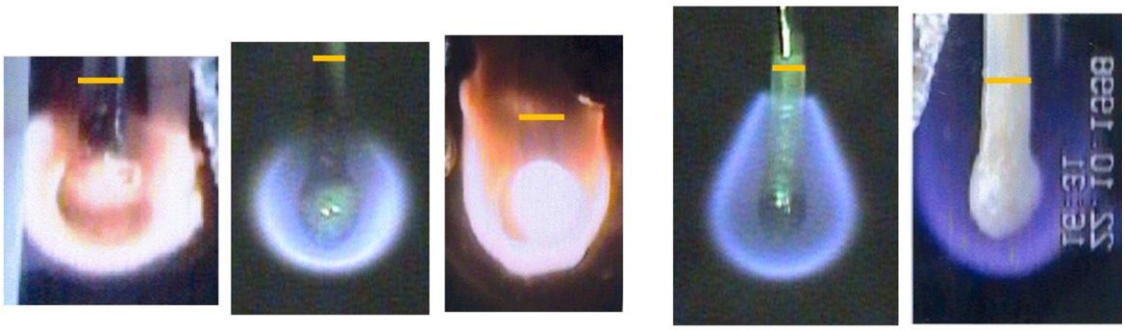

a) b) c) d) e)

Figure 19. A comparison between flames during long duration experiments performed on the Mir space station [13], with the short drop tests reported here. Flame magnifications adjusted to match using rod diameter as a scale; the Mir tests were 4.5 mm diameter rods and the drop tests were 3.175 mm diameter rods. Other environment variables noted below.
Extruded PMMA: a) Mir test in 22.3% O_2 at 2 cm/s; b) drop test in 21% O_2 at 5 cm/s; c) Mir test in 25.4% O_2 at 8.5 cm/s.
POM: d) drop test in 21% O_2 at 5 cm/s. e) Mir test in 25.4% O_2 at 7 cm/s;

flame spread and more like bulk regression of the rod. So it seems clear that the preferred mode of combustion of materials under ISS ventilation flow conditions is for the flame to move to stabilize on the upwind-most end of the material and burn backward from there. This is consistent with results with thin charring fuels as well [16, 17].

Lastly, downstream soot deposition was noted in some of the PMMA drop tests. This soot, if thick enough, could suppress subsequent burning of the material beneath the soot layer, but for thin coatings could enhance burning by increasing absorption. Thus sooting conditions should be minimized during testing since it is desired to re-use samples for multiple tests. For near-limit testing, this should be less of a problem in microgravity, since flames generally turn all blue near the extinction limit [16, 17].

In order to fairly compare extinction limits from NASA's Upward Flame Propagation Test 1 with future flight experiment extinction limits, the effect of smaller sample size and geometry on extinction limits needs to be evaluated, so that the appropriate samples can be tested on orbit. A series of 5.18 second Zero Gravity Research Facility drop tests is reported which compare the effect of geometry on the flame size, shape, and stability over two different materials in the form of flat slabs, spheres, and rods under otherwise identical atmospheric conditions (The International Space Station atmosphere of 14.7 psia, 21% oxygen). Flames generally quickly reached a steady flame size, and in one instance, growing flame size. Overall flame lengths were 15-25 mm, flame widths were 18-22 mm, and standoff distances were 3-8 mm. Length to width ratios were on the order of unity, and flame standoff to sample radius ratios were on the order of 1-3. The growing flame was spreading over the rod at 1.1 mm/s, slower than the 1g spread rate of 1.85 mm/s. Burning behavior noted with these fuels included sample warping, bending, and the development of a molten ball at the end of the rod. Significant bubbling and swelling was also noted with POM and extruded PMMA for all geometries. Of the materials tested, cast PMMA appears to best maintain its shape for repeated testing. Sooting conditions should be minimized to avoid downstream deposition that may affect desired repeated testing with the same sample. Only preliminary extinction limit data has been obtained to date. In future testing, we will evaluate how sensitive the flammability limits are to geometry changes.

1.3 Knowledge Lacking

For fire research, NASA currently tests materials for flammability using NASA STD-6001 Test 1, which is a normal gravity upward burning test. Unfortunately, recent testing has shown that this test may not be conservative for some materials that burn better in microgravity under spacecraft ventilation flow conditions. Ground-based microgravity facilities do not provide enough microgravity time to study all but the thinnest of fuels (tissue paper, plastic films). The solid phase response time of real materials is too long to ignite them in ground-based tests, let alone let them reach steady-state burning or demonstrate flammability limits.

NASA Test 1 samples have a 6" burn length criterion, and there is currently no way to directly do comparable tests in microgravity. The 2011 Decadal Survey highlighted this technology gap and called for "Improved methods for screening materials in terms of flammability in space environments will enable safer space missions. Present tests, performed in normal gravity, are not adequate for reduced gravity scenarios."

2.0 Flight Experiment

2.1 Objectives and hypothesis of the flight investigation

First and foremost, we seek to develop a fundamental understanding of how NASA's material flammability test, NASA-STD-6001.A Test 1, relates to the actual flammability of materials in low- and partial-gravity. As part of this goal, we will obtain a better fundamental understanding of material flammability as a function of concurrent flow, oxygen, and pressure.

Rather than a pass/fail criteria, the modified Test 1 procedure will measure an actual materials flammability limit information that reflects both the lowest oxygen concentration at which a flame can propagate 6" and the highest oxygen concentration at which a flame will extinguish within 6".

The hypothesis to be tested in this research is that a material's flammability hazard in microgravity or partial gravity is at least equivalent to and may be greater than its flammability measured in normal gravity. We also hypothesize that most materials exhibit a similar flammability boundary as a function of oxygen and flow. These two hypotheses then imply that there may be a similar magnitude negative oxygen margin of safety for many materials. If true, a common factor of safety is could be defined for materials to 'de-rate' them for use in microgravity or partial gravity.

We also hypothesize that the boundary of the concurrent flammability map is essentially a limit dictated by the critical heat flux for ignition, where the heat flux from the flame is insufficient to sustain the burning. As was shown in [Olson et al., 2006], the limiting opposed flow flame spread velocity is directly related to the critical heat flux for ignition. This may also be true for concurrent flame spread. This implies that there is a fixed limiting spread rate along the flammability boundary.

2.2 Objectives, Science Data End Products, and Requirements

2.2.1 Objective 1

To obtain the lower portion of the concurrent microgravity flammability map for select materials as a function of ventilation flow, ambient oxygen concentration, and *possibly* pressure, to find the minimum oxygen concentration (MOC) on the map over the range of interest for spacecraft exploration atmospheres.

Sub-Objective a: Measure the flammability limits of a ***non-charring material*** as a function of forced concurrent flow velocity and oxygen concentration, all at 1 atm.

Science Data End Product

Graph of flammability boundary with flow velocity and oxygen concentrations as axes.

The MOC will be identified from this map.

Sub-Objective b: Measure the flammability limits of a ***charring material*** as a function of forced concurrent flow velocity and oxygen concentration, all at 1 atm.

Science Data End Product

Graph of flammability boundary with flow velocity and oxygen concentrations as axes. The MOC will be identified from this map.

Sub-Objective c: (desired) Measure the flammability limits of a base material (TBD) as a function of forced concurrent flow velocity and oxygen concentration, ***at a reduced pressure associated with exploration atmospheres.***

Science Data End Product

Graph of flammability boundary with flow velocity and oxygen concentrations as axes. The MOC will be identified from this map.

2.2.2 Objective 2

To obtain the lower portion of the *opposed* microgravity flammability map for a TBD material as a function of ventilation flow, and ambient oxygen concentration to determine if opposed or concurrent flow has the lower minimum in microgravity. It is often assumed that the concurrent limit will be at a lower oxygen concentration than the opposed because that is how it is in normal gravity. However, given the flame's tendency to spread upwind instead of downwind near the limit in microgravity, this may not be the case in microgravity. The lower of the two limits will be defined as the worst case in microgravity.

Note: if other investigators are willing to collaborate, the opposed map from their testing could be compared to the same material in the concurrent flow regime from this testing.

Science Data End Product

Graph of flammability boundary with opposed flow velocity and oxygen concentrations as axes. The MOC will be identified from this map.

Requirements: TBD similar to above, depending on material selected (one of the 2 above). Flow direction relative to ignition end is reversed. There will be holder changes.

2.2.3 Objective 3

To compare worst case materials flammability limits in microgravity to modified NASA 6001 Test 1 MOC limits to evaluate the oxygen margins of safety for the materials.

Science Data End Product: An evaluation of the minimums in the flammability maps from Objective 1 compared to ground-based 1g Test 1 limits for the same materials. Oxygen margins of safety will be calculated using

$$\Delta O_2\%_{0g-1g} = \left(\frac{(0gULOI + 0gMOC}{2}\right) - \left(\frac{(1gULOI + 1gMOC}{2}\right) \quad Eqn(1)$$

In addition, this oxygen margin of safety will be compared with the oxygen margin of safety estimated from ground-based drop tower testing to determine the conservatism of drop testing in evaluating 0g limits.

2.3 Anticipated Knowledge to be Gained, Value, and Application

This data can be used to compare with real use environment oxygen conditions so an 'oxygen factor of safety' can be used to rank the candidate materials for an application. A material with higher oxygen factor of safety is clearly better.

Microgravity and partial gravity materials flammability limits will be quantified for specific materials, and an 'oxygen margin of safety' will be added to the normal gravity 'oxygen factor of safety' to better reflect the materials actual fire performance in space. Data to date suggests this 'margin of safety' is on average -2% oxygen (for flow velocities of 30 cm/s, or at lunar g levels), but can be up to -6% oxygen. This is a *negative* margin of safety. This implies that NASA Test 1 is *not* conservative and materials should be de-rated by this margin of safety.

The flammability boundary (Figure 13 concept) will provide information on the sensitivity to ventilation flow on the margin of safety. The velocity threshold limits can be compared with computational fluid dynamics of spacecraft ventilation velocities will identify spacecraft zones where ignition could more likely lead to flame propagation, and allow preventive actions (flow redirection, selecting materials with adequate factors of safety; optimizations of extinguishers placement, etc.).

Pressure effects on oxygen and ventilation flammability threshold limits will be examined. Characterization of pressure/oxygen/ventilation effects in normal gravity and microgravity will allow building multi-dimensional flammability threshold models capable of predicting flammability behavior within the acceptable spacecraft breathable limits, and allow safe transitions from one set of spacecraft conditions to another. We will also be able to evaluate flammability risks in emergency situations. Selecting better materials will allow designing realistic fire extinguishment systems. In the long term, the flammability threshold technique will lead to understanding parametric effects on aerospace materials flammability and thus allow adequate management of spacecraft fire risks.

3.0 EXPERIMENT REQUIREMENTS

3.1 Science Requirements Summary Table

Objective 1a and 1c Requirements:

1. Fuel material – cast polymethylmethacrylate
2. Fuel sample is a cylinder of sufficient length to support steady state regression of the rod slowly so flow can be incrementally changed without extinguishing and reigniting between flows.
3. Rod dimensions are ~20 cm long (15 cm = 6" Test 1 criteria), total initial length x 0.635 cm diameter. Multiple rods will be flown.
4. The fuel rod will be held in a sleeve that can expose the desired amount of fuel while protecting the rest from heat and soot inside. Holder sleeve will be made of low conductivity non-flammable material with an inner surface coated with a layer of low friction material (possibly Delrin). Thickness of the sleeve is less than 1/16". The sleeve will have a scale painted on it longitudinally, and the diameter will serve as the orthogonal scale, marked with a ring that is visible in the ambient chamber lighting. The fuel will be remotely deployed as needed from this sleeve. The initial length of exposed fuel at ignition will be ~ 7 cm. The ignition tip will be near the center of the field of view of the imaging systems.
5. The holder sleeve will have at least one temperature sensor on it to determine if the tip of the sleeve is reaching the glass transition pmma temperature (115^{o}C). The fuel sample will be deployed by 1 cm increments at a reasonable speed during a burn (~0.5 cm/s extrusion rate) to keep the temperature at the tip of the sleeve below this temperature so the pmma does not stick inside the sleeve. In addition, this sensor will determine cool-down times. An additional gas-phase temperature protruding forward from the sleeve is also needed to detect the proximity of the flame to the tip of the sleeve, since the sleeve will have a slow response time during the combustion tests. At least 15 cm of the rod should be deployable. The rod should be replaceable in the sleeve, or the entire sleeve replaceable.
6. The tip of the fuel rod should be exposed to a uniform steady flow that extends at least 3.5 cm on all sides of the rod. There should be no flow obstruction in the ~7 cm diameter x 8 cm long flow 'cylinder' around the exposed rod.
7. A retractable igniter is needed to ignite the tip of the fuel. Once retracted, the igniter must be at least 3.5 cm away from the rod. A kanthal hot wire igniter has worked well in the past, operating at ~ 3.7 amps. The igniter should be easily replaceable, with a number of spares, since they are prone to breakage.
8. Flow system capable of velocities between 0.5 and 30 cm/s.
9. Flow field must be laminar and uniform to within 1 cm/s or better, with better uniformity desired at the lower flows. The flow should be characterized using hot wire anemometer profiling in at least 2 orthogonal orientations.
10. Flow ramping specification: The flow will be changed in discrete steps of 2 cm/s with fine-tuning at the minimum in the map of 1 cm/s steps. The flow should respond to the step change in no less than 1 second and no more than 5 seconds. The flame

must spread for longer than the solid-phase response time before changing flow again, since we have seen in BASS that concurrent spread is a function of the heating history of the fuel, especially in the decreasing flow direction. This should not be difficult for low flows where the flame is small, but can be problematic for higher flow tests where the flame is long.

11. Flow should be measured at one point in proximity to the test sample, but so as to not disturb the flow near the burning tip. Suggest: 2 cm away from the sleeve at the plane of the sleeve opening for verification, or alternatively at 3 cm upstream and 3 cm radially from the tip of the rod. (Suggested technique: hot wire, etc.)
12. Vessel to achieve conditions (oxygen 10% to 21%, pressure 14.7 psia)
13. Initial oxygen concentration specified to +/- 0.005 mole fraction.
14. Initial pressure specified to +/- 0.1 psia.
15. Color video of flame (sensitive to dim blue, at a minimum rate of 5 Hz. Camera field of view 10 cm perpendicular to rod x 10 cm parallel to rod, with tip of offset so the edge of the holder sleeve is just in the edge of the field of view. Image resolution 0.01 cm).
16. Backlit view of rod to measure regression rate of the rod. Color image to see the flame and the backlit rod simultaneously. Framing rate 1 Hz. Field of view is 5 cm orthogonal rod and 5 cm parallel to the rod, with the initial rod location centered orthogonally but shifted upstream so 1.5 cm upstream of the tip and 3.5 cm downstream of the tip are imaged. Image resolution is 0.005 cm.
17. Backlight should be adjustable in brightness, and uniformly diffuse to within 5 8-bit gray levels over the camera field of view. It should not interfere with orthogonal imaging of the flame. Backlight color: suggest green leds (wavelength tbd).
18. Sensors to measure the test atmosphere oxygen concentration of the flow upstream and downstream of sample. Oxygen concentration measured at tbd Hz and accurate to 0.005 mole fraction. Gas from the flow duct should be well mixed at the sensor downstream of the sample to provide a good average measure of the oxygen consumption when compared with the upstream reading, which is assumed to be well mixed.
19. Sensors to measure the test atmosphere pressure of the flow upstream of sample. Pressure measured at 10 Hz and accurate to 0.1 psia.
20. Sensors to measure flow velocity upstream of sample. Accuracy and precision are specified as…TBD.
21. Sensors to measure flow temperature upstream of sample. Accuracy and precision are specified as…TBD.
22. CO and CO2 sensors are desired to measure the incompleteness of combustion. Gas from the flow duct should be well mixed at the sensors' location downstream of the sample to provide a good average measure.

23.

24. Chamber should be dark and nearby objectives should be diffuse black to minimize stray light reflection.

25. Different colored chamber lights (leds) should be available to verify set-up (e.g. igniter position), fuel condition, or ambient light during test. (Suggest independently controlled RGB for white total or colored).

26. All data should have a time-stamp that can be correlated to the video time stamps.

Objective 1b and 1c Requirements

27. Fuel material – tbd charring fabric. Candidates: SIBAL fuel, cheesecloth, Nomex III

28. Fuel sample is a flat sheet of fabric held flat with the upstream edge exposed and the other 3 sides held in a low-conductivity holder.

29. Sample sheet exposed area is at least 15 cm long (15 cm = 6" Test 1pass/fail criteria) total length x 5 cm wide. Multiple sheets will be flown, built in to sample holders with integral igniters.

30. The sample holder will be made of a low conductivity non-flammable material. The holder will be as thin as possible to maintain a flat profile in 0g for a color edge view, on the order of the fuel thickness itself. The holder should be easily accessed for change out, since each sample is a one-time use. The holder will be centered in the field of view of the imaging systems. The width of the holder will be 7 cm, and the length will be ~16 cm. The samples should be held firmly. A thin kapton tape has worked well for ground-based testing. This option leaves open the possibility to refurbish the cards on orbit, and there is precedent for this.

31. The holder will have scales marked in both x and y directions around the perimeter of the holder, in the field of view of the top camera. At the downstream end a scale will be attached that is perpendicular to the plane of the sample (like a fin) that will appear in the orthogonal camera field of view

32. The upstream edge of the sample should be exposed to a uniform steady flow that extends at least 1 cm past each side of the sample (7 cm total). There should be no flow obstruction in the ~7 cm diameter x 8 cm long flow 'cylinder' around the sample holder.

33. A built-in igniter is needed to ignite the upstream edge of the fuel. A kanthal hot wire igniter has worked well in the past, operating at ~ 3.7 amps. Each sample card will have an igniter. They should be replaceable in case of breakage or card refurbishment.

34. Flow system capable of velocities between 0.5 and 30 cm/s.

35. Flow field must be laminar and uniform to within 1 cm/s or better, with better uniformity desired at the lower flows. The flow should be characterized using hot wire anemometer profiling in at least 2 orthogonal orientations.

36. Flow ramping specification: The flow will be changed in discrete steps of 2 cm/s with fine-tuning at the minimum in the map of 1 cm/s steps. The flow should respond to the step change in no less than 1 second and no more than 5 seconds. The flame must spread over more than the preheated fuel length before changing flow again, since we have seen in BASS that concurrent spread is a function of the heating history of the fuel, especially in the decreasing flow direction. This should not be difficult for low flows where the flame is small, but can be problematic for higher flow tests where the flame is long.
37. Flow should be measured at one point in proximity to the test sample, but so as to not disturb the flow near the sample. Suggest: 3 cm above the sample holder plane at 4 cm upstream of the leading edge of the sample card. (Suggested technique: hot wire, etc.)
38. Vessel to achieve conditions (oxygen 10% to 30%, pressure 14.7 psia)
39. Initial oxygen concentration specified to +/- 0.005 mole fraction.
40. Initial pressure specified to +/- 0.1 psia.
41. Color video of flame (sensitive to dim blue, at a rate of 10 Hz. Camera field of view 8 cm perpendicular to holder (side view) x 17 cm parallel to holder, with holder centered in the field of view. Image resolution 0.02 cm).
42. Surface-lit view of sample holder to measure pyrolysis front and burnout front of the sample with time. Color image (sensitive to dim blue) to see the flame and the pyrolysis front simultaneously. Framing rate 10 Hz. Field of view is 7 cm across holder and orthogonal rod and 17 cm along the sample holder, with the holder centered in the field of view. 0.02 cm.
43. Sample lighting should be adjustable in brightness, and uniformly illuminating the sample diffuse to within 5 8-bit gray levels over the camera field of view. It should not interfere with orthogonal imaging of the flame. Light color: suggest green leds (wavelength TBD).
44. Sensors to measure the test atmosphere oxygen concentration of the flow upstream and downstream of sample. Oxygen concentration measured at TBD Hz and accurate to 0.005 mole fraction. Gas from the flow duct should be well mixed at the sensor downstream of the sample to provide a good average measure of the oxygen consumption when compared with the upstream reading, which is assumed to be well mixed.
45. Sensors to measure the test atmosphere pressure of the flow upstream of sample. Pressure measured at 10 Hz and accurate to 0.1 psia.
46. Sensors to measure flow velocity upstream of sample. Accuracy and precision are specified as…TBD.
47. Sensors to measure flow temperature upstream of sample. Accuracy and precision are specified as…TBD.

48. CO and CO2 sensors are desired to measure the incompleteness of combustion. Gas from the flow duct should be well mixed at the sensors' location downstream of the sample to provide a good average measure.
49.
50. Chamber should be dark and nearby objectives should be diffuse black to minimize stray light reflection.
51. Different colored chamber lights (leds) should be available to verify set-up (e.g. igniter position), fuel condition, or ambient light during test. (Suggest independently controlled RGB for white total or colored).
52. All data should have a time-stamp that can be correlated to the video time stamps.

Objective 2 Requirements:

TBD pending discussion with other PIs. The opposed flow map would be obtained for either the selected charring or non-charring fuel. Other than ignition at the opposite end of the fuel, the other requirements would be similar to those above.

Objective 3 Requirements:

There are no flight requirements for this objective. There are requirements for ground-based testing to evaluate the limits in normal gravity.

3.2 Detailed discussion of the requirements and their justification

Note: this section seems to be largely redundant to that above. I need some guidance as to what is expected where……perhaps the above section is this section, and you just want a table above?

3.2.1 Experiment Configuration

The experiment configuration required is a flow system with the fuel sample suspended in that flow stream and ignited.

3.2.2 Experimental Operating Conditions

Ambient pressure test will vary oxygen % in nitrogen and flow velocity to find the flammability map.

3.2.3 Experimental Monitoring Measurements

Color imaging of the flame and either backlight imaging or surface-lit imaging of fuel surface are required. Oxygen concentration will be measured. See above.

3.2.4 Experimental Diagnostics

See above.

3.2.5 Operational Requirements (data, possible operational approach)

Video data to determine if the flame extinguishes or not is required prior to the next tests. Some time is needed (1 hour) to quickly determine from video tracking if the flame is steady or not. Test condition data is also required prior to the next test. The oxygen and flow velocity parameters will be varied in increments approaching the flammability boundary.

3.2.6 Microgravity Requirement

Microgravity levels need to be low enough than any residual buoyant flow is less than 0.5 cm/s, so flammability limits can be found in the diffusive region as well as where convective flow dominates. For Vb ~ 30 $g^{1/3}$, this give g< 10^{-6} g.

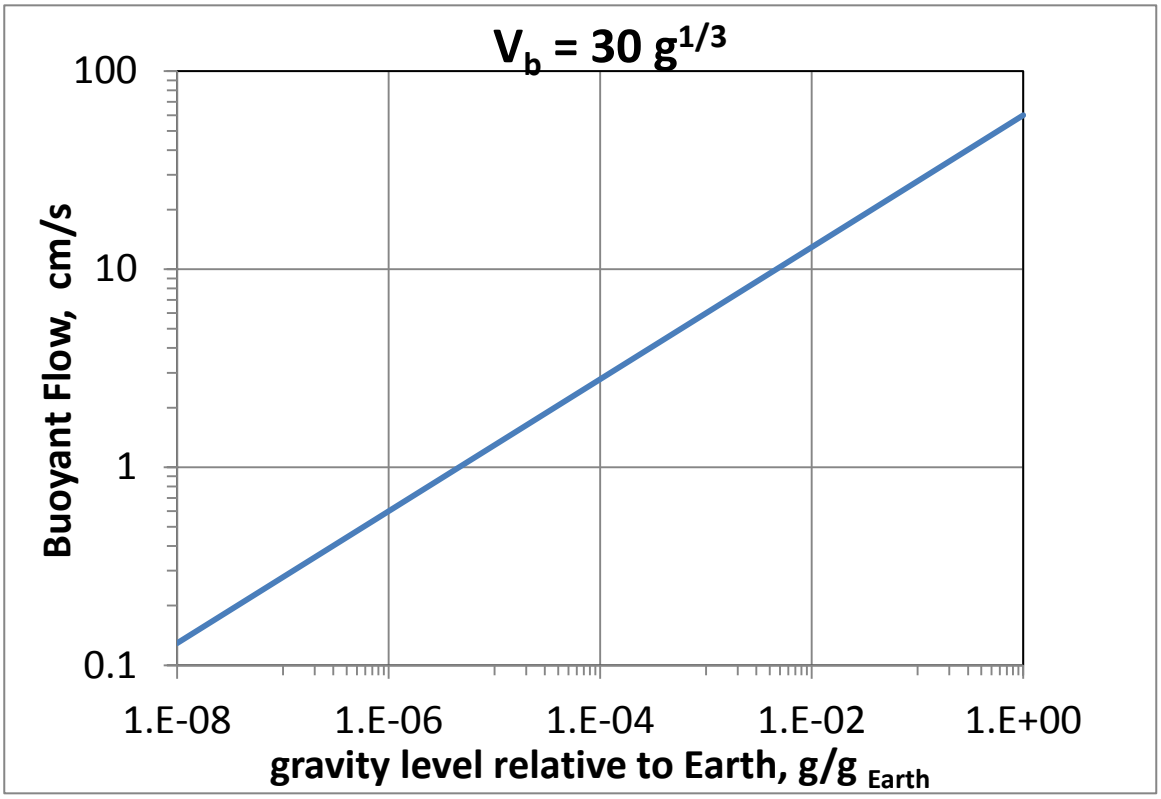

3.3 Detailed test matrix

Note that the actual values in the following table are placeholders in the range of expected values. Ground-based testing will help fine tune the oxygen and flow velocity ranges for each matrix.

Objective 1a: non-charring material

Quenching boundary points have priority over blowoff boundary points, which will be traded off if more quench points are needed.

Samples will be ignited at a flammable flow condition, and then the flow changed to the matrix values, multiple 'test points' can be conducted in one burn for the pmma rods. The number of ignitions would be a minimum of each of the 8 O_2 values x2 (repeat of the limit) = 16, or a maximum of 33. It is recommended that enough igniters are flown to provide a new igniter for every test point (i.e. 33 retractable igniters)

While most tests will be performed at constant oxygen concentration and changing flow, once the minimum O2 and flow are found in this way, it is desired to run a test at constant flow and slowly decreasing oxygen concentration to determine the minimum oxygen concentration at the minimum in the flammability map.

#	Fuel	O2, mole%	Flow, cm/s
1	PMMA	17	6
2			4
3			2
4			1
5			Repeat limit flow, 1 cm/s increment
6		16	6
7			4
8			2
9			1
10			Repeat limit flow, 1 cm/s increment
11		15	6
12			4
13			2
14			Repeat limit flow, 1 cm/s increment
15		14	4
16			2
17			Repeat limit flow, 1 cm/s increment
18		14	6
19			8
20			10
21			Blowoff-2cm/s
22			Repeat limit flow, 1 cm/s increment
23		15	5
24			10
25			15
26			Blowoff-2 cm/s
27			Repeat limit flow, 1 cm/s increment
28		16	10
29			15
30			20
31			Repeat limit flow, 1 cm/s increment
32		Min, decreasing	Min value on flammability boundary
33			Repeat min

Objective 1b: charring material

Quenching boundary points have priority over blowoff boundary points, which will be traded off if more quench points are needed.

Samples will be ignited at a flammable flow condition, and then the flow changed to the matrix values, It may be possible for multiple 'test points' with one sample if the material burns slowly enough and the flames are not long. However, to be conservative, one flow per sample is required. Each sample will have an integral igniter.

While most tests will be performed at constant oxygen concentration and changing flow, once the minimum O2 and flow are found in this way, it is desired to run a test at constant flow and decreasing oxygen concentration to determine the minimum oxygen concentration at the minimum in the flammability map. The decrease will have to be performed more quickly than for the PMMA. Estimates of the vititation rate are 1% O2 change within the flame spread time.

#	Fuel	O2, mole%	Flow, cm/s
1	Fabric	17	6
2			4
3			2
4			1
5			Repeat limit flow, 1 cm/s increment
6		16	6
7			4
8			2
9			1
10			Repeat limit flow, 1 cm/s increment
11		15	6
12			4
13			2
14			Repeat limit flow, 1 cm/s increment
15		14	4
16			2
17			Repeat limit flow, 1 cm/s increment
18		14	6
19			8
20			10
21			Blowoff-2cm/s
22			Repeat limit flow, 1 cm/s increment
23		15	5
24			10
25			15
26			Blowoff-2 cm/s
27			Repeat limit flow, 1 cm/s increment
28		16	10
29			15
30			20
31			Repeat limit flow, 1 cm/s increment
32		Min, decreasing	Min value on flammability boundary
33			Repeat min

Objective 1c (desired): tbd base material

Testing at a reduced pressure of 8 psia and 10.2 psia. The flammability boundary will shift upward in O_2. The testing will be conducted the same way as the 1 atm pressure tests. the testing will result in 3 minimums at the 3 pressures over the range of interest for exploration atmospheres.

10.2 psia matrix:

#	Fuel	O2, mole%	Flow, cm/s
1	TBD, PMMA or Fabric	19	6
2			4
3			2
4			1
5			Repeat limit flow, 1 cm/s increment
6		18	6
7			4
8			2
9			1
10			Repeat limit flow, 1 cm/s increment
11		17	6
12			4
13			2
14			Repeat limit flow, 1 cm/s increment
15		16	4
16			2
17			Repeat limit flow, 1 cm/s increment
18		18	6
19			8
20			10
21			Blowoff-2cm/s
22			Repeat limit flow, 1 cm/s increment
23		17	5
24			10
25			15
26			Blowoff-2 cm/s
27			Repeat limit flow, 1 cm/s increment
28		16	10
29			15
30			20
31			Repeat limit flow, 1 cm/s increment
32		Min, decreasing	Min value on flammability boundary
33			Repeat min

8 psia matrix:

#	Fuel	O2, mole%	Flow, cm/s
1	TBD, PMMA or Fabric	19	6
2			4
3			2
4			1
5			Repeat limit flow, 1 cm/s increment
6		18	6
7			4
8			2
9			1
10			Repeat limit flow, 1 cm/s increment
11		17	6
12			4
13			2
14			Repeat limit flow, 1 cm/s increment
15		16	4
16			2
17			Repeat limit flow, 1 cm/s increment
18		18	6
19			8
20			10
21			Blowoff-2cm/s
22			Repeat limit flow, 1 cm/s increment
23		17	5
24			10
25			15
26			Blowoff-2 cm/s
27			Repeat limit flow, 1 cm/s increment
28		16	10
29			15
30			20
31			Repeat limit flow, 1 cm/s increment
32		Min, decreasing	Min value on flammability boundary
33			Repeat min

Objective 2: tbd base material

Testing at opposed flow to find the minimum in the flammability boundary for comparison with the concurrent minimum. This will allow us to determine what is the worst case condition for microgravity flame spread.

Multiple flow points for a single burn are much simpler for opposed flow. The flame spread only needs to occur for the preheat time of the solid phase at each flow condition. However, the hardware should include one sample per test point..

Note: if other investigators are willing to collaborate, the opposed map from their testing could be compared to the same material in the concurrent flow regime from this testing, making these test points unnecessary for this investigation.

#	Fuel	O2, mole%	Flow, cm/s
1	TBD, PMMA or Fabric	19	6
2			4
3			2
4			1
5			Repeat limit flow, 1 cm/s increment
6		18	6
7			4
8			2
9			1
10			Repeat limit flow, 1 cm/s increment
11		17	6
12			4
13			2
14			Repeat limit flow, 1 cm/s increment
15		16	4
16			2
17			Repeat limit flow, 1 cm/s increment
18		18	6
19			8
20			10
21			Blowoff-2cm/s
22			Repeat limit flow, 1 cm/s increment
23		17	5
24			10
25			15
26			Blowoff-2 cm/s
27			Repeat limit flow, 1 cm/s increment
28		16	10
29			15
30			20
31			Repeat limit flow, 1 cm/s increment
32		Min, decreasing	Min value on flammability boundary
33			Repeat min

3.4 Success Criteria

Definitions:

Complete success: achievement of all peer reviewed objectives
Signiificant success: achievement of the most important or a significant fraction of the objectives
Minimal success: achievement of a single objective or collection of enough data to produce a paper published in an archival journal.

3.4.1.1 Science success Criteria

3.4.1 Minimal Success

The minimum in the concurrent flammability map is identified for one material, to compare with the 1g flammability limit and determine the oxygen margin of safety for that material. Flame measurements are made that determine if the flame is steady or not at each test condition.

3.4.2 Significant Success

The minimum in the concurrent and opposed flow flammability maps are obtained for the same material, allowing the identification of the worst case flow configuration for microgravity fires. The oxygen margin of safety will be defined based upon that minimum. Flame measurements are made that determine if the flame is steady or not at each test condition. Heat release and fuel consumption measurements are obtained for the tests.

3.4.3 Complete Success

The minimum in the concurrent and opposed flow flammability maps are obtained for the same material, allowing the identification of the worst case flow configuration for microgravity fires. The oxygen margin of safety will be defined based upon that minimum.

The minimum in the concurrent flammability map is identified for the second material, to compare with the 1g flammability limit and determine the oxygen margin of safety for that material.

(Desired) The minimum in the flammability map is determined at 3 pressures so that the effect of pressure in the exploration atmosphere range can be assessed , to see if there is a pressure correlation that can be developed..

Flame measurements are made that determine if the flame is steady or not at each test condition. Heat release and fuel consumption measurements are obtained for the tests. (Desired: CO/CO2 data is compared with global stoichiometry estimates to determine the incompleteness of combustion as the limits are approached.

3.4.2 Hardware success Criteria

3.4.2.1 Minimal Success

For one material's concurrent test matrix: The flow and oxygen variables are well controlled and monitored with sensors to provide verification of appropriate test conditions. The fuel sample is properly

positioned for ignition and imaging. Flame imaging is adequate to determine flame extinction. The igniters are adequate to ignite the flame.

3.4.3 Significant Success

For one material's concurrent and opposed test matrix: The flow and oxygen variables are well controlled and monitored with sensors to provide verification of appropriate test conditions. The fuel sample is properly positioned for ignition and imaging. Flame imaging is adequate to determine flame extinction. The igniters are adequate to ignite the flame. Backlit or surface lit images provide a measure of the fuel consumption rate, and the oxygen sensors provide a measure of the oxygen consumption rate to evaluate the heat release rate and global stoichiometry for each test as we approach the flammability limit.

3.4.4 Complete Success

For nearly all tests (90+% of required matrix) :The flow and oxygen variables are well controlled and monitored with sensors to provide verification of appropriate test conditions. The fuel sample is properly positioned for ignition and imaging. Flame imaging is adequate to determine flame extinction. The igniters are adequate to ignite the flame. Backlit or surface lit images provide a measure of the fuel consumption rate, and the oxygen sensors provide a measure of the oxygen consumption rate to evaluate the heat release rate and global stoichiometry for each test as we approach the flammability limit.

4.0 JUSTIFICATION FOR EXTENDED DURATION MICROGRAVITY ENVIRONMENT

4.1 Limitations of Terrestrial (1g laboratory) Testing

For most configurations and dimensions, the buoyant flow around the flame on Earth is such that the buoyant flow is too high to mimic the ventilation flows of interest for spacecraft fire safety applications, or even buoyant flow on the Moon or Mars. For concurrent flame spread in particular, the normal gravity upward flame spread rate is significant, and steady-state is difficult to obtain except for very narrow fuel samples. Previous work, shown in Figure 21, has shown that a minimum oxygen concentration in the concurrent flammability map [Jiang] occurs at reduced gravity and at reduced ventilation flows (minimum O2 at < 10 cm/s forced flow) relative to normal gravity buoyant flows, which are typically in excess of 30 cm/s.

4.2 Limitations of Drop Towers and Aircraft

Flammability limits are very difficult to obtain in the limited time available in ground-based facilities. Drop towers are limited to 5.18 seconds, and aircraft g-jitter is to high and varied (10-2g ~ 10

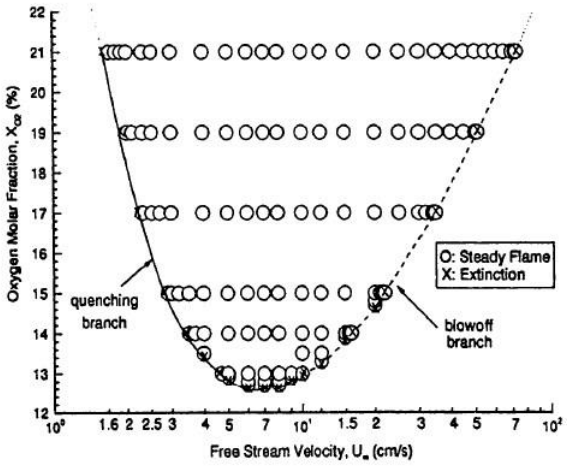

Figure 21: Computed concurrent flame flammability map for forced flow [Jiang].

cm/s flow, fluctuations on the order of seconds) to make aircraft suitable for flammability testing.

4.3 Need for Accommodations in the Space Station, Space Shuttle, or Sounding Rocket

Judicious selection of very thin fuels can improve the ground-based accessible parameter space, but ultimately a flight experiment will be needed for practical thicknesses of materials, and to verify the ground-based microgravity and partial gravity results.

4.4 Limitations of Modeling Approaches

Detailed computational modeling of flammability boundaries relies on many assumptions about fuel and flame properties, and for real materials many of these are not known, such as pyrolysis kinetics, gas-phase fuel species, and gas-phase chemical reaction mechanisms. Near-limit flames are very sensitive to difficult to quantify heat losses to the fuel holder, radiative exchange between the flame and fuel surface, and radiative loss to the surroundings. These unknowns add up to large uncertainties in the predicted limits and mechanisms of extinction.

5.0 Science Management Plan

Post Flight Data analysis Plan

The color flame images and backlit or surface lit images will be analyzed using flame tracking software. The PI has extensive experience with this tracking, as exemplified in the many flame tracking graphs in the introduction section. Flame size, shape (length, width, standoff distance), and spread rate / regression rate will be tracked with time to determine if the flame is steady at the test conditions. The steady values will be compared between tests to observe trends with the control variables and as the flame approaches extinction.

The digital data will be plotted to show time trends and comparisons between tests. Oyxgen consumption data will be used to determine heat release rate using Huggett's constant. Trends in heat release with the control variables and as the flame approaches extinction will be observed.

Fuel consumption rates measured from video tracking will be compared to oxygen consumption to determine global stoichiometry. This will be compared to CO and CO2 sensor data If they are available. Trends in the data with the control variables and as the flame approaches extinction will be observed.

6.0 References and Citations (alphabetical order)

Bhattacharjee, S., Altenkirch, R.A., and Sacksteder, K.; *J. Heat Transfer* 118, 181-190, (1996).

Campbell, P.D., JSC-63309, "Recommendations for Exploration spacecraft Internal Atmospheres: The Final Report of the NASA Exploration Atmospheres Working group", (January 2006).

Di Blasi, C., Fire Mater. 22, 95-101, (1998).

Ferkul, P.V. "An Experimental Study of Opposed Flow Diffusion Flame Extinction Over a Thin Fuel in Microgravity", NASA CR 182185, (Feb. 1989).

Ferkul, P.V.; "A Model of Concurrent Flow Flame Spread Over a Thin Solid Fuel", NASA CR-191111, 1993.

Feier, I.I., Kleinhenz, J., T'ien, J.S., Ferkul, P.V., and Sacksteder, K. "Pressure Modeling of Upward Flame Spread Rates in Partial Gravity",43rd AIAA Aerospace Sciences Meeting and Exhibit, 10 - 13, Reno, Nevada, (January, 2005).

Ferkul, P.V., and Olson, S.L.; "Zero-Gravity Centrifuge Used for the Evaluation of Material Flammability in Lunar-Gravity", *Journal of Thermophysics and Heat Transfer*, V. 25, No. 3, (2011) pp. 457-461; also presented at the 40th International Conference on Environmental Systems, July 11-15, 2010, Barcelona, Spain.

Grayson, G., Sacksteder, K.R., Ferkul, P.V., and T'ien, J.S.; Microgravity Science and Technology, 11 (2) 187-195, (1994).

Hirsch, D.B, and Beeson, H.D., "Improved Test method to Determine Flammability of Aerospace Materials," Halon Options Technical Working Conference (24-26 April 2001).

Hirsch, D.B., and Beeson, H.D. "Test Method to Determine Flammability of Aerospace Materials," Journal of Testing and Evaluation V.30, Issue 2, (4 pages), (March, 2002).

Hirsch, D.B, Williams, J.H, Harper, S.A., Beeson, H., and Pedley, M.D.; "Oxygen Concentration Flammability Thresholds of Selected Aerospace Materials considered for the Constellation program," Second IAASS Conference: Space Safety in a Global World, Chicago, Illinois, (May 2007).

Hirsch, D.B, Williams, J., and Beeson, H.; "Pressure Effects on Oxygen Concentration Flammability Thresholds of Polymeric Materials for Aerospace Applications" Journal of Testing and Evaluation, V.36, Issue 1, (pp. 69-72). NASA Document ID 20070018178, (2008).

Hirsch, F. Juarez, S. Motto, S. Harper, and S. Olson' "Selected Parametric Effects on Materials Flammability Limits", 41st International Conference on Environmental Systems (ICES), 17–21 July 2011, Portland, OR.

Huggett, Clayton. 1980. Estimation of rate of heat release by means of oxygen consumption measurements. *Fire and Materials*. **4**(2), pp.61-65.

Jiang, Ching-Biau; "A Model of Flame Spread over a Thin Solid in Concurrent Flow with Flame Radiation", Ph.D. Dissertation, Case Western Reserve University, 1995.

Kleinhenz, J.E., "Flammability and Flame Spread of Nomex and Cellulose in Space Habitat Environments", Ph.D. Dissertation, CWRU, (May 2006).

Klimek, R. and Wright, T.; Spotlight image analysis software, http://microgravity.grc.nasa.gov/spotlight/, (2005).

Lewis, J.F, Barido, R.A, and Tuan, G. “Crew Exploration Vehicle Environmental Control and Life Support Fire Protection Approach,” International Conference on Environmental Systems, SAE 2007-01-3255, (July 2007).

Magee, R. S. and McAlevy III, R. F. ; J. Fire & Flammability, 2, 271-297, (1971).

NASA CxP 70024, Revision A, Change 001, Constellation Program Human-Systems Integration Requirements, Oct. 30, 2007.

NASA STD-6001, *Flammability, Odor, Offgassing, and Compatibility Requirements and Test Procedures for Materials in Environments that Support Combustion,*, Test **1,** Upward Flame Propagation, (formerly NHB 8060.1C), (February 9, 1998).

Olson, S.L.; The Effect of Microgravity on Flame Spread Over a Thin Fuel, NASA TM-100195, (1987).

Olson, S. L., Ferkul, P.V., and T'ien, J.S.,;"Near-Limit Flame Spread Over a Thin Solid Fuel in Microgravity", *Twenty-Second Symposium (International) on Combustion*, The Combustion Institute, pp. 1213-1222, (1988).

Olson, S.L.; *Combustion Science and Technology* 76 (4-6), 233-249, (1991).

Olson, S.L., Beeson, H.D., Haas, J.P., and Baas, J.S.; “An Earth-Based Equivalent Low Stretch Apparatus for Material Flammability Assessment in Microgravity and Extraterrestrial Environments”, Proceedings of the Combustion Institute, Vol 30/2 pp 2335-2343, 2005.

Olson, S. L., Miller, F. J., and Wichman, I. S., “Characterizing Fingering Flamelets Using the Logistic Model,” *Combustion Theory and Modelling 10(2), pp 323-347,* (2006).

Olson, S.L., Ruff, G., and Miller, F.J., “Microgravity Flame Spread in Exploration Atmospheres: Pressure, Oxygen, and Velocity Effects on Opposed and Concurrent Flame Spread”, 08ICES-0147, presented at the International Conference On Environmental Systems, July, 2008, San Francisco, CA. Also NASA TM-2008-215260, 2008.

Olson, S.L., Griffin, D.W., Urban, D.L., Ruff, G.A., and Smith, E.A.; “Flammability of Human Hair in Exploration Atmospheres”, 09ICES-0168, International Conference on Environmental Systems, Savannah, GA, July, 2009.

Olson, S.L. and Ruff, G.A.; “Microgravity Flame Spread over Non-Charring Materials in Exploration Atmospheres: Pressure, Oxygen, and Velocity Effects on Concurrent Flame Spread”, 09ICES-0167, International Conference on Environmental Systems, Savannah, GA, July, 2009.

Olson, S.L. and Miller, F.J., “Experimental Comparison of Opposed and Concurrent Flame Spread in a Forced Convective Microgravity Environment”, Proceedings of the Combustion Institute, V. 32, 2445-2452, 2009.

Olson, S.L. and Ferkul, P.V. “Evaluating Materials Flammability in Microgravity and Martian Gravity Compared to NASA’s Normal Gravity Materials Flammability Testing”, 42st International Conference on Environmental Systems (ICES), 15-19 July 2012, San Diego, CA.

Olson, S.L. and Hirsch, D. “Geometry Considerations in Evaluating 0g Materials Flammability Limits for Comparison with NASA Test 1 Limits”, 41st International Conference on Environmental Systems (ICES), 17–21 July 2011, Portland, OR.

Pettegrew, R. D.; ‘An Experimental Study of Ignition Effects and Flame Growth over a Thin Solid Fuel in Low-Speed Concurrent Flow Using Drop-Tower Facilities’, NASA CR

198537, (Oct. 1996).

Sauers, D.G.; "The Effects of Forced Air Flow and Oxygen Concentration on Flammability, Smoke Density, and Pyrolytic Toxicity", J. Fire Flammability, V. 7, pp. 181-199, (1976).

7.0 APPENDICES

7.1 Modeling Status/Description

7.2 Validation / demonstration of diagnostic systems

7.3 On-going ground-based work to support RDR and beyond.